UNCLASSIFIED

[redacted]

WADC TECHNICAL REPORT 52-34, PART 1

[redacted]

AUTOGENOUS ELECTRIFICATION OF A B-45A AIRCRAFT

Part 1. Preliminary Investigation

CARL A. BARTELT
COMMUNICATION AND NAVIGATION LABORATORY

DECEMBER 1951

WRIGHT AIR DEVELOPMENT CENTER

UNCLASSIFIED

NOTICES

When Government drawings, specifications, or other data are used for any purpose other than in connection with a definitely related Government procurement operation, the United States Government thereby incurs no responsibility nor any obligation whatsoever; and the fact that the Government may have formulated, furnished, or in any way supplied the said drawings, specifications, or other data, is not to be regarded by implication or otherwise as in any manner licensing the holder or any other person or corporation, or conveying any rights or permission to manufacture, use, or sell any patented invention that may in any way be related thereto.

The information furnished herewith is made available for study upon the understanding that the Government's proprietary interests in and relating thereto shall not be impaired. It is desired that the Judge Advocate (WCJ), Wright Air Development Center, Wright-Patterson Air Force Base, Ohio, be promptly notified of any apparent conflict between the Government's proprietary interests and those of others.

WADC TECHNICAL REPORT 52-34, PART 1

AUTOGENOUS ELECTRIFICATION OF A B-45A AIRCRAFT

Part 1. Preliminary Investigation

Carl A. Bartelt
Communication and Navigation Laboratory

December 1951

RDO No. 112-28

Wright Air Development Center
Air Research and Development Command
United States Air Force
Wright-Patterson Air Force Base, Ohio

McGregor & Werner, Inc.
Dayton, O. 100, 25 Nov. 52

FOREWORD

This report was prepared by the Communication and Navigation Laboratory, Weapons and Components Division, Wright Air Development Center. Work reported herein was accomplished under Research and Development Order R112-28, "Suppression of Precipitation Static." This is the first report of a series to be issued on this project; later reports will be published as the research progresses.

Personnel of Communication and Navigation Laboratory who participated in the project were: Mr. P. W. Couch, Project Engineer; Mr. C. A. Bartelt, who performed flight tests, reduced and analyzed data and prepared the report; and Mr. Q. J. Porter, who rendered much valuable assistance in calibration and maintenance of instruments and reduction of data.

Flight Test Division, Wright Air Development Center, provided crews and maintenance for the test aircraft. Without their wholehearted cooperation, the research described in this report would have been impossible.

[redacted]

ABSTRACT

The problem of precipitation static is becoming increasingly severe with present-day high-speed aircraft. The use of large transparent plastic surfaces with various antenna mounted under the plastic surface accentuates the problem. A B-45A type aircraft was instrumented to measure the electrostatic condition of the aircraft and the canopies in flight. Eleven flights have been made through atmospheric conditions varying from clear air to high-altitude snow and ice crystals at temperatures of -20 to -40°C. Tentative conclusions reached are that precipitation static generated on the canopy is serious. Instrumentation problems for research on electrification of canopies have been resolved, and quantitative evaluation of surface treatments to reduce canopy precipitation static may now be accomplished. The electrostatic characteristics of the aircraft as a whole have been determined over a very limited range of magnitudes.

The security classification of the title of this report is UNCLASSIFIED.

PUBLICATION REVIEW

This report has been reviewed and is approved.

FOR THE COMMANDING GENERAL:

for Robert E. Kates
CHARLES U. BROMBACH
Colonel, USAF
Chief, Comm and Nav Laboratory
Directorate of Laboratories

[redacted]

TABLE OF CONTENTS

	Page
SECTION I - INSTRUMENTATION	1
SECTION II - TESTS AND TEST RESULTS	15
SECTION III - CONCLUSIONS	37

LIST OF ILLUSTRATIONS

Figures		Page No.
1	Block Diagram of Complete Installation, less Noise-Meter	2
2	External View of Nose of Test Aircraft Showing Aluminum Charging Patches	3
3	External View of Nose of Test Aircraft Showing Canopy Current Collectors	4
4	External View of Top of Test Aircraft Showing Electric Field Meter Detector Head	5
5	External View of Belly of Test Aircraft Showing Electric Field Meter Detector Head	5
6	Internal View of Test Aircraft Looking out through Nose Section	6
7	External View of Test Aircraft Showing Liaison Antenna	6
8	External View of Pilot's Canopy of Test Aircraft	7
9	Internal View of Pilot's Canopy of Test Aircraft	7
10	Outside View of Noise Pickup Probes Installed in Nose Canopy	8
11	Installation of Noise Pickup Probes in Nose Canopy	8
12	Block Diagram of Noise Meter Installation	9
13	Internal View of Nose of Test Aircraft	10
14	Installation of Special Noise Meter and Associated Equipment in Nose Compartment	11
15	Sample Oscillograph Record	12
16	Data Analyzer MX-(XA-123)/U	13

LIST OF ILLUSTRATIONS (Cont'd)

Figures		Page No.
17	Variplotter (Electronics Associates, Inc., Model 205B) and Data Analyzer MX-(XA-123)/U	14
18	Top Electric Field as a Function of Charging Current	15
19	Bottom Electric Field as a Function of Charging Current	16
20	Bottom Electric Field as a Function of Charging Current	17
21	Top Electric Field as a Function of Charging Current	18
22	Top Electric Field as a Function of Canopy Charging Current	20
23A	Top Electric Field as a Function of IAS	21
23B	Top Electric Field as a Function of IAS on Log Log Coordinates	21
24	Top Electric Field as a Function of Bottom Electric Field	23
25	Top Electric Field as a Function of Bottom Electric Field	24
26	Liaison Antenna Corona Current as a Function of Bottom Electric Field	25
27	Nose Electric Field as a Function of Canopy Charging Current	26
28	Nose Electric Field as a Function of Canopy Charging Current-time Product	27
29	Nose Electric Field as a Function of IAS	28
30	Canopy Charging Current as a Function of IAS	29
31	Canopy Charging Current as a Function of IAS	30
32	Left Canopy Collector Current as a Function of Right Canopy Collector Current	31

LIST OF ILLUSTRATIONS (Cont'd)

Figures		Page No.
33	Left Canopy Collector Current as a Function of Right Canopy Collector Current	32
34	Left Canopy Collector Current as a Function of Right Canopy Collector Current	33
35	Radio-frequency Noise on the Canopy as a Function of Nose Electric Field	34
36	Radio-frequency Noise on the Canopy as a Function of Nose Electric Field	35

INTRODUCTION

Many unsatisfactory reports have been received about precipitation static in Radio Compass AN/ARN-6. In many instances the precipitation static is severe enough to render the compass useless. This is particularly true of jet aircraft having large plastic canopies. Some of the types of aircraft affected by this interference are the F-86, F-94, B-45, and the B-47.

One of the first attempts to measure electrostatic charging of jet aircraft was made at Air Materiel Command in November 1944, using a P-59A type aircraft. The instrumentation was damaged in flight, and no data were obtained. Initial ground calibration and flights were started in January 1948, on an FP-80A which had been instrumented at Air Materiel Command. One flight was made through low-altitude rain, and no measurable charging was observed. The airplane crashed at the conclusion of this flight, and the airplane and instrumentation were destroyed.

Reports were received of severe precipitation static interference in radio receivers on the YB-49 in May 1948. An electric field meter, and a meter to measure trailing wire corona current were installed in a YB-49 in June 1948, and a flight was made in clear air. No measurable fields were observed, and with the trailing wire extended 150 feet, there was no measurable trailing wire corona current. A second F-80 was instrumented in 1949 and 1950 and 36 flights were made through snow and ice crystals. The data are in process of analysis at this writing.

Specific details about which more complete information was sought are: the effect of jet exhausts on the net charge on the aircraft, effects of electrostatic charging of the canopies, and data on charging current to the aircraft as a function of true air speed for air speeds greater than 300 MPH.

A B-45A, serial number 47-014, was received at Wright-Patterson Air Force Base on 7 August 1950, and installation of equipment for precipitation static research was initiated on that date. The instrumentation passed inspection on 18 September 1950, and the first flight was made on 2 October 1950.

SECTION I - INSTRUMENTATION

The aircraft has been instrumented to measure, and record continuously, 16 quantities as a function of time. The quantities to be measured are:

(1) Charging current to any two combination of four aluminum patches mounted on the radome, on the nose of the aircraft.

(2) Charging current to each of three sections of the transparent nose canopy. These three sections will hereafter be called "canopy collectors," or just "collectors."

(3) Corona current from each of two antennas.

(4) Radio-frequency noise inside the nose canopy, under either of two symmetrically located canopy current collectors.

(5) Corona current from each of the two noise probes.

(6) Electrostatic field at two points on the surface of the aircraft.

(7) Electrostatic field under the nose canopy, presumably caused by electrostatic charge on the canopy.

(8) Altitude.

(9) Indicated air speed.

(10) An audio-frequency voltage from the voice recorder for synchronizing the voice and oscillograph records.

A more detailed description of the instrumentation with block diagrams and photographs follows.

The initial installation was made without the noise meter and noise probes, which were added at a later date. Figure 1, page 2, is a block diagram of the instrumentation without the noise meter. Input signals which were too small in magnitude to deflect the remote meters and galvanometers were amplified. The output of the electric field meter detector heads is a 400-cps sinusoidal voltage, proportional in magnitude to the magnitude of the electric field, and in phase or 180° out of the phase with a reference voltage, in accordance with the polarity of the applied electric field. A detector-amplifier circuit is necessary to convert the signal to a d-c voltage which changes in magnitude and sign, in accordance with the electric field, for the remote meters and galvanometers. The operation of all circuits used in this instrumentation is described in the second report in this series, Autogenous Electrification of a B-45A Aircraft, II Instrumentation, Q. J. Porter, WADC Technical Report Number 52-34.

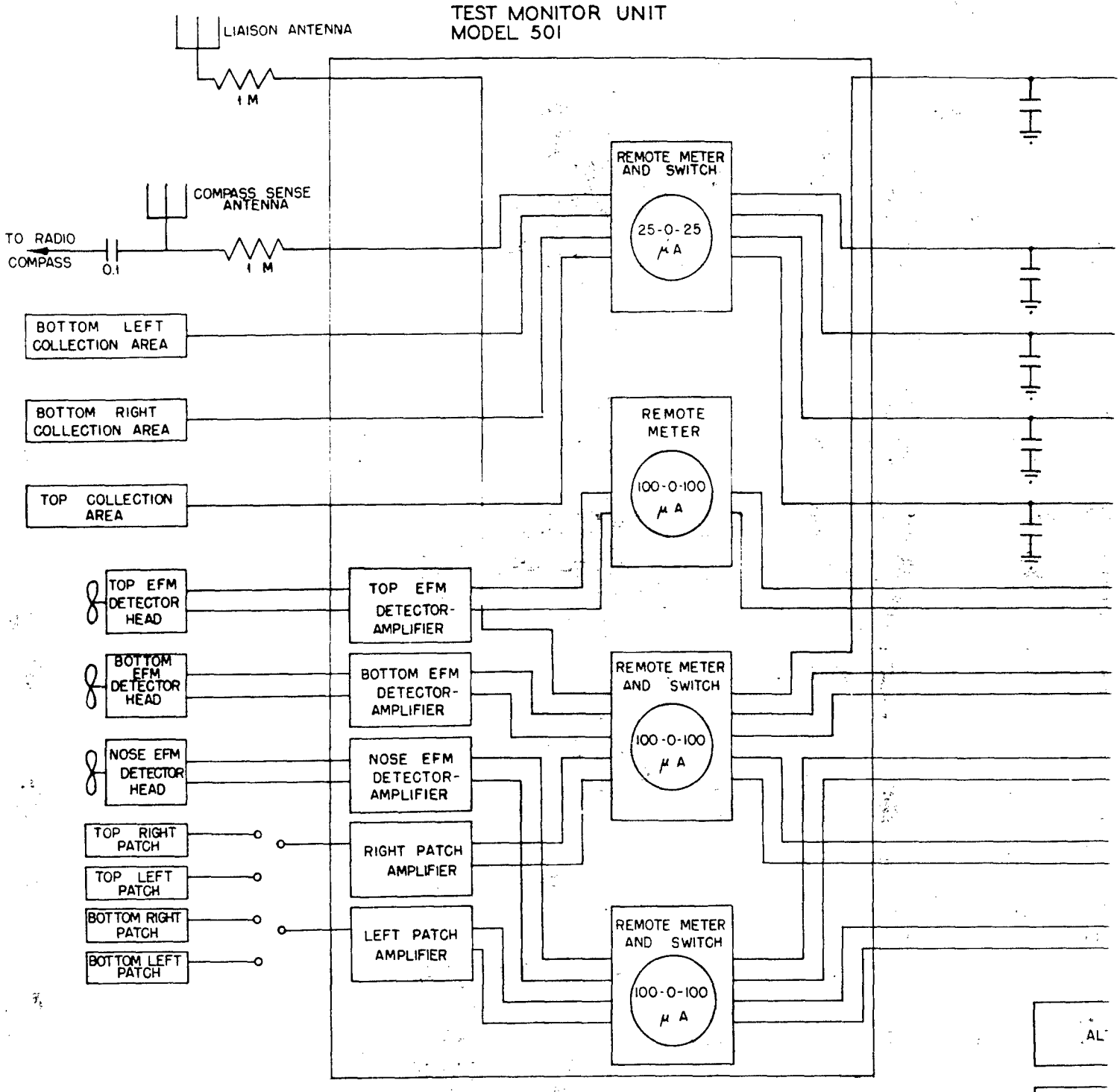

Figure 1
Block Diagram of the Complete Installation, Less Noise Meter

[redacted]

CONSOLIDATED ENG. CORP.
RECORDING OSCILLOGRAPH
TYPE 5-114 P3

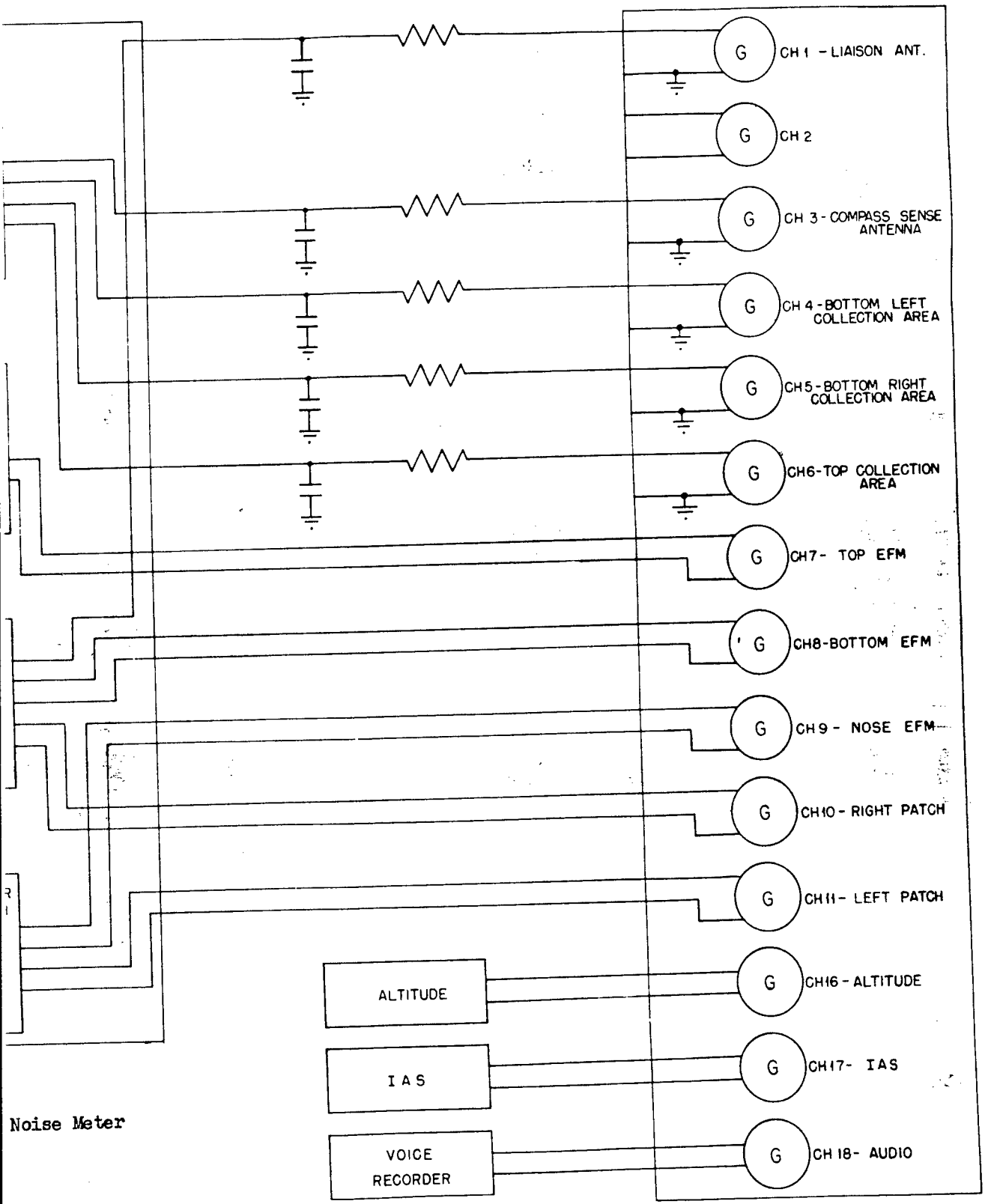

Noise Meter

[redacted]

2

An 18-channel recording oscillograph is used to continuously monitor all 16 quantities which are being measured. Remote meters are installed to permit an observer to monitor any 4 out of 10 preselected quantities during a test. Switches are used in conjunction with the remote meters to permit the observer to select which 4, out of the 10, quantities he wishes to monitor during any given test.

Four aluminum patches were used to measure charging current to the aircraft. Figure 2, and Figure 3, page 4, show the physical installation of these patches on the aircraft.

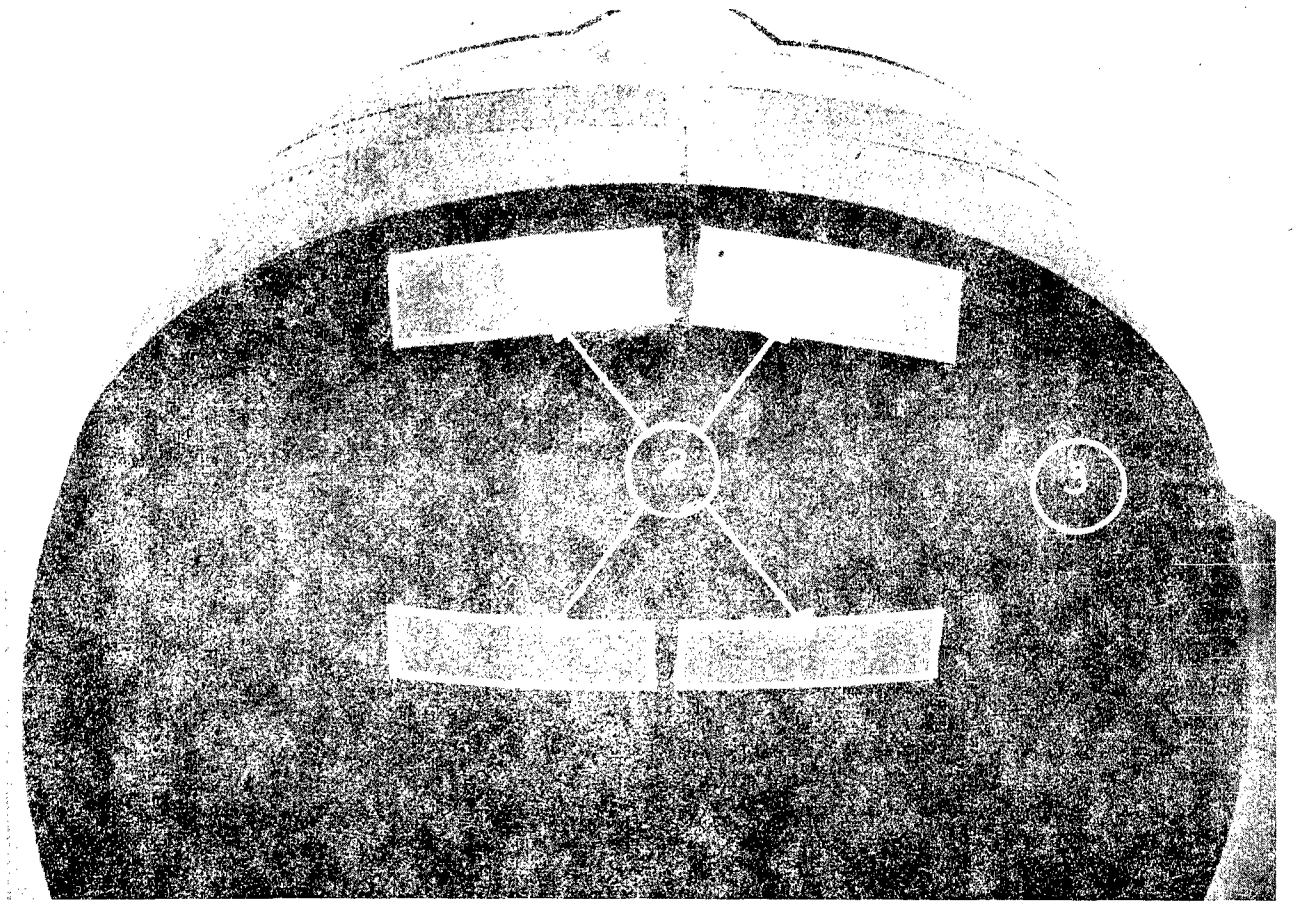

Figure 2
External View of Nose of Test Aircraft

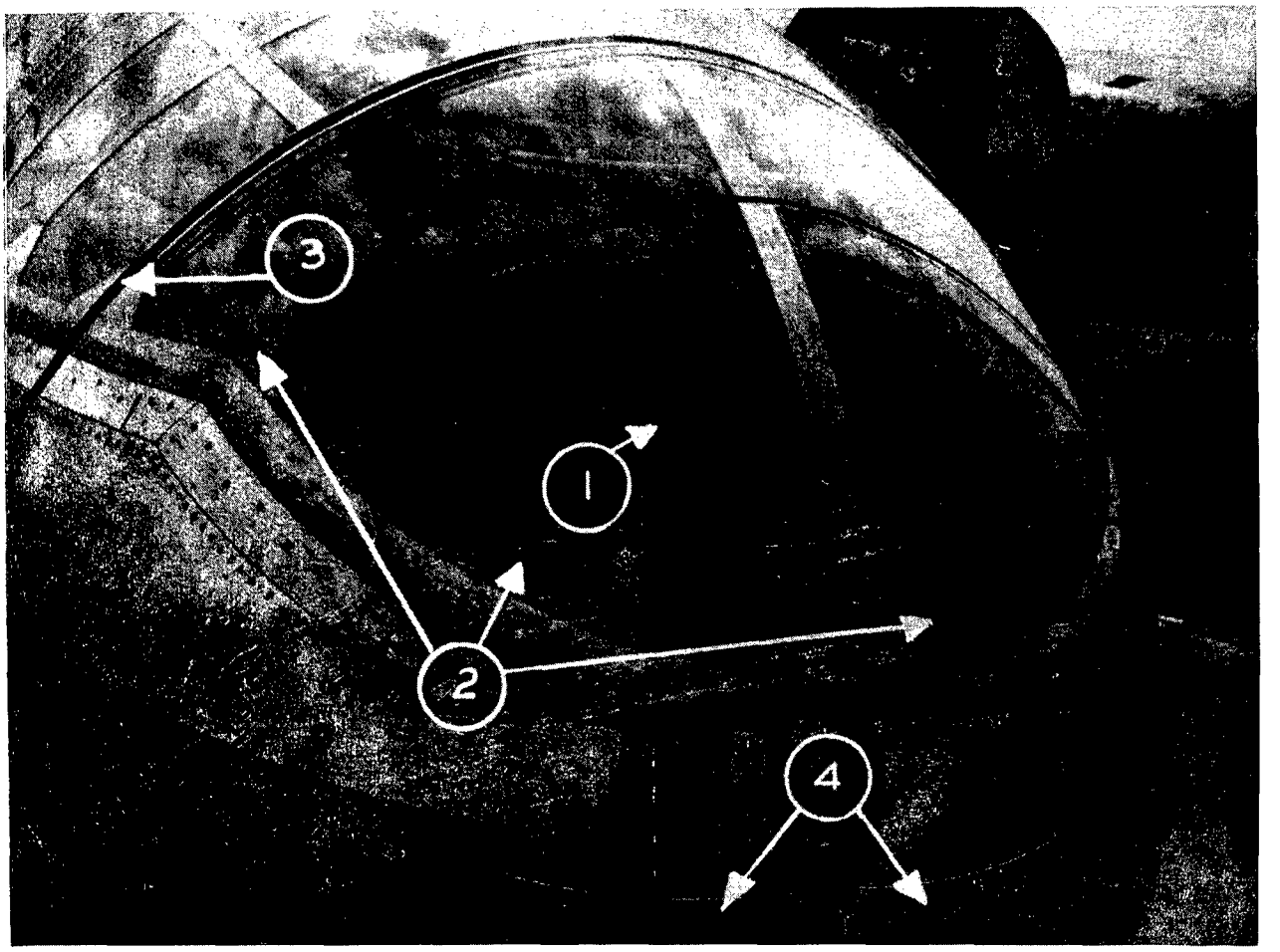

Figure 3
External View of Nose of Test Aircraft

They were mounted to permit checking the effect of angle of incidence, and symmetry of charging about the longitudinal axis of the aircraft. Any combination of the four patches could be applied to the two patch amplifiers to permit testing the effect of different angles of incidence, and different projected frontal areas. Unfortunately, after several flights had been made, leakage paths developed across the insulated band around the patches, rendering much of the patch current data of doubtful significance.

Electrostatic field, caused by charge built up on the aircraft, is measured at two points on the surface of the aircraft. One electric field meter detector head is located near the center of gravity, and on top of the aircraft, as shown in Figure 4, page 5. The other one is located on the bottom of the aircraft, approximately halfway between the after tunnel hatch, and the tail

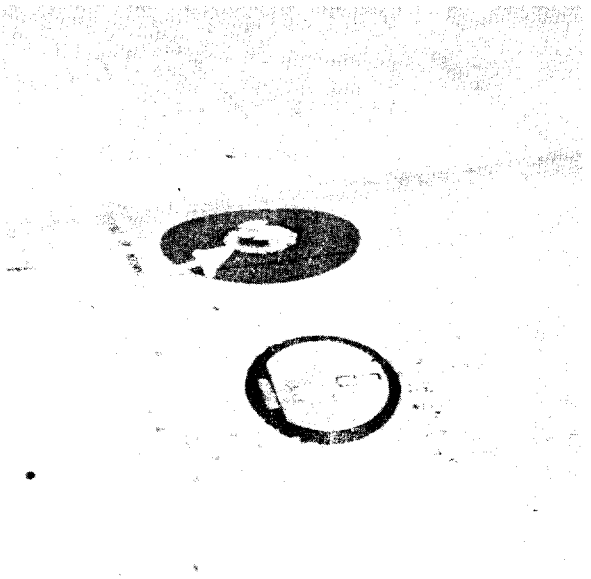

Figure 4
External View of Top of Test Aircraft Showing Electric Field Meter Detector Head

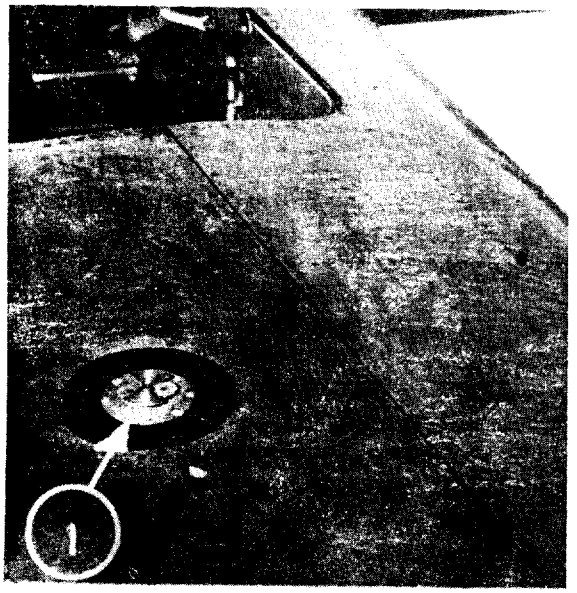

Figure 5
External View of Belly of Test Aircraft Showing Electric Field Meter Detector Head

bumper, as shown in Figure 5. Two electric field meters were used to give a cross check between the two, and to help distinguish between exogenous and autogenous charging. The electrostatic field meter under the nose canopy measures the field caused by the electrostatic charge on the outside of the canopy. The location of the detector head is shown in Figure 3, page 4.

Two of the canopy collection areas were made as nearly symmetrical as possible about the longitudinal axis of the aircraft, in an effort to get identical data from two sections of the canopy. These collection areas are shown in Figure 5, and Figure 6, page 6. These data were desired in order to have one "standard" collection area, and one collection area for testing formulas for reducing canopy charging. The third collection area is much larger than the two symmetrical ones, and has a much lower angle of incidence. It is used to provide a cross check on the other two, and to check charging effects at low angles of incidence.

Corona currents from two antennas were measured to give an indication of the amount of radio-frequency noise attributable to that source. Corona currents from the liaison and compass sense antennas were measured, and recorded. The liaison antenna was chosen because of its highly exposed (electrostatically) location, and also, because of the high susceptibility of the liaison receiver to precipitation static. This is well illustrated in Figure 7, page 6. The radio compass is also highly susceptible to precipitation static. Although the compass sense antenna is completely buried in the pilot's canopy, it also was monitored for corona current. Figures 8 and 9, page 7, show internal and external views of the section of

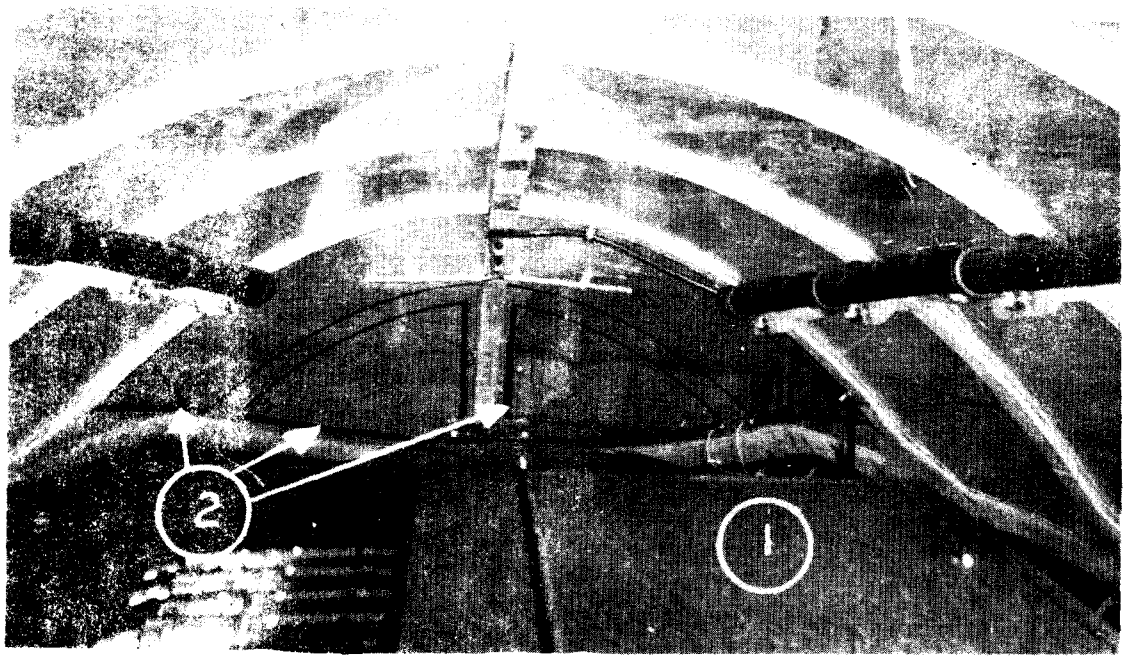

Figure 6
Internal View of Test Aircraft, Looking Out Through Nose Section.

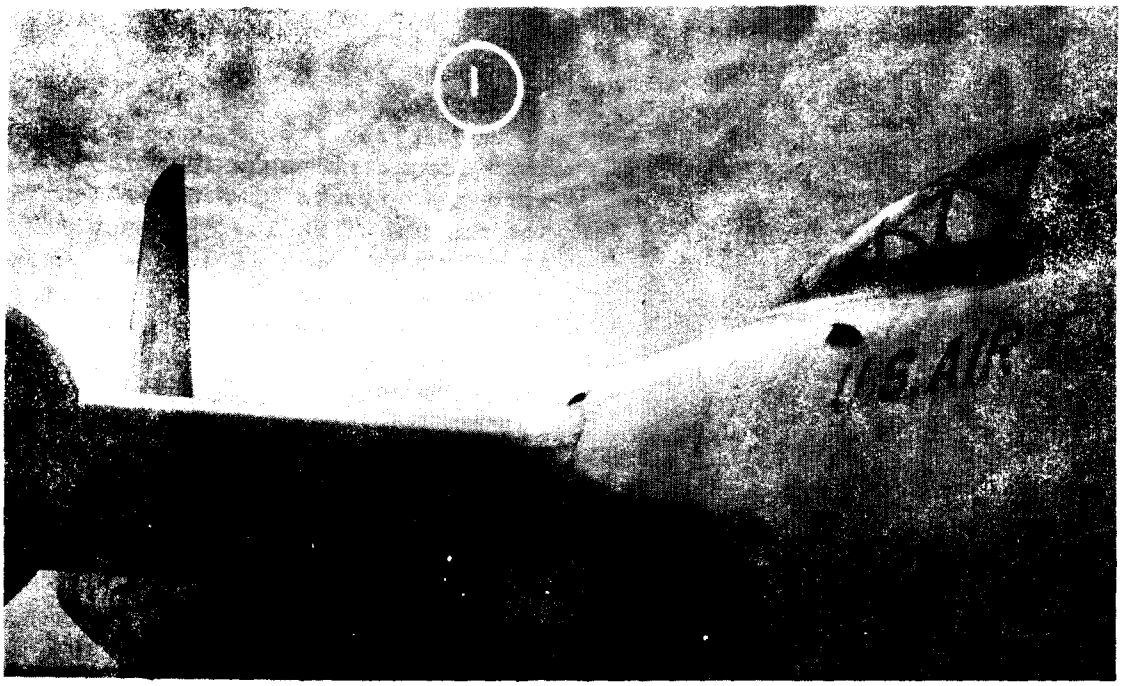

Figure 7
External View of Test Aircraft Showing Liaison Antenna

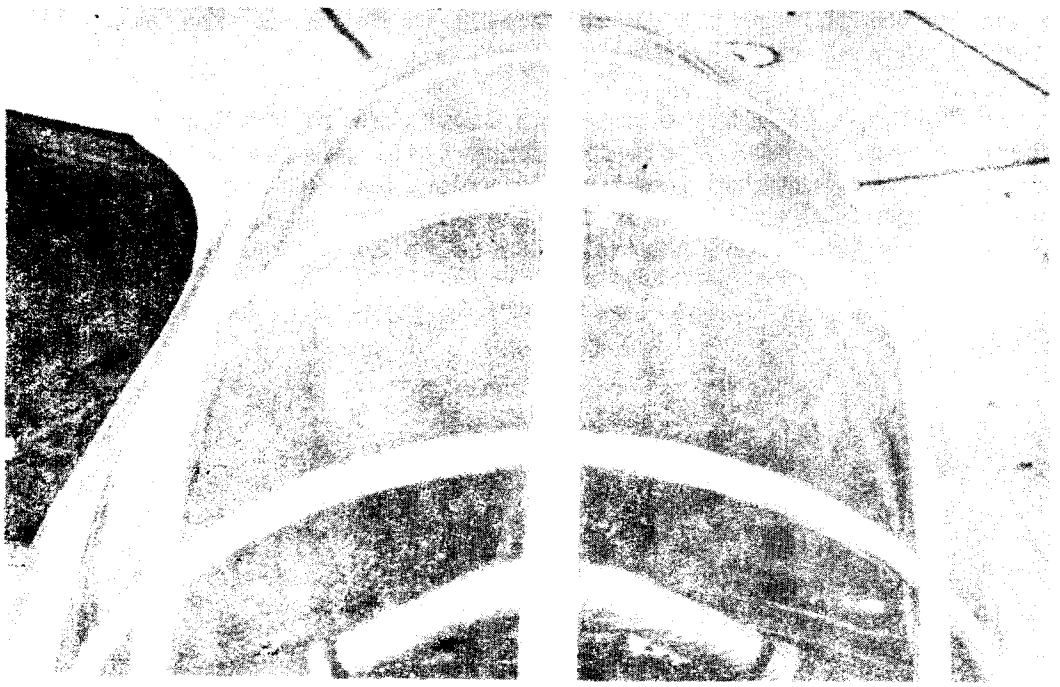

Figure 8
External View of Pilot's Canopy of Test Aircraft

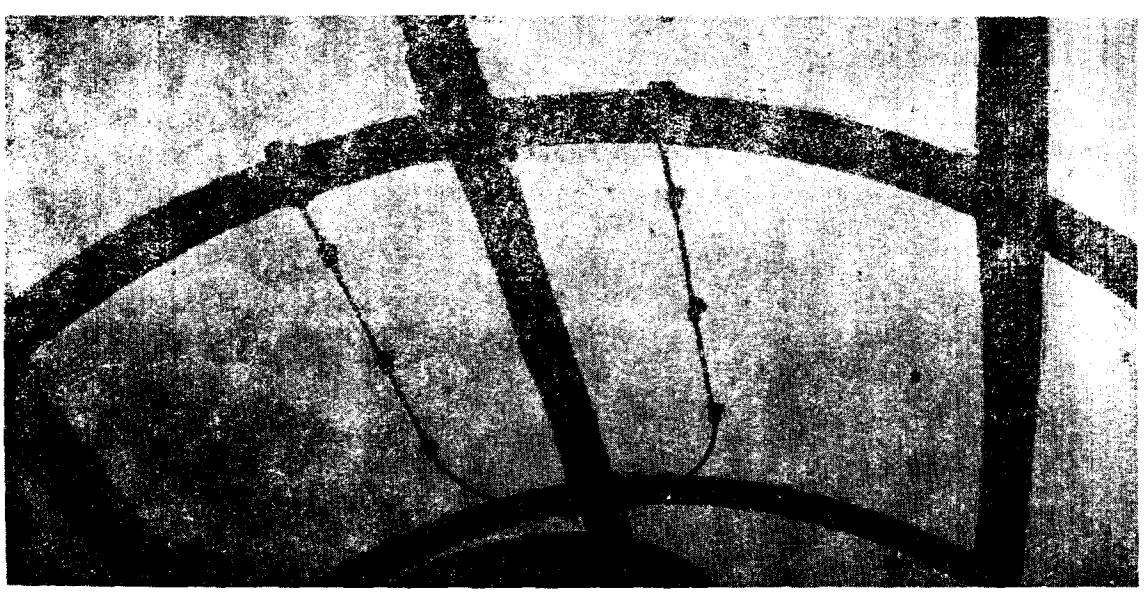

Figure 9
Internal View of Pilot's Canopy of Test Aircraft

the pilot's canopy which contains the sense antenna. The "U" shaped antenna showing in the photographs is the localizer antenna. The sense antenna is buried in several of the Fiberglas ribs.

An RCA type 312B noise meter was installed in the interval between flight numbers six and seven. Radio-frequency noise was measured on either one of two noise probes mounted immediately under the two symmetrical collection areas. Figures 10 and 11 show the installation of the noise probes. A coaxial switch is used to select the noise probe to be monitored by the noise meter.

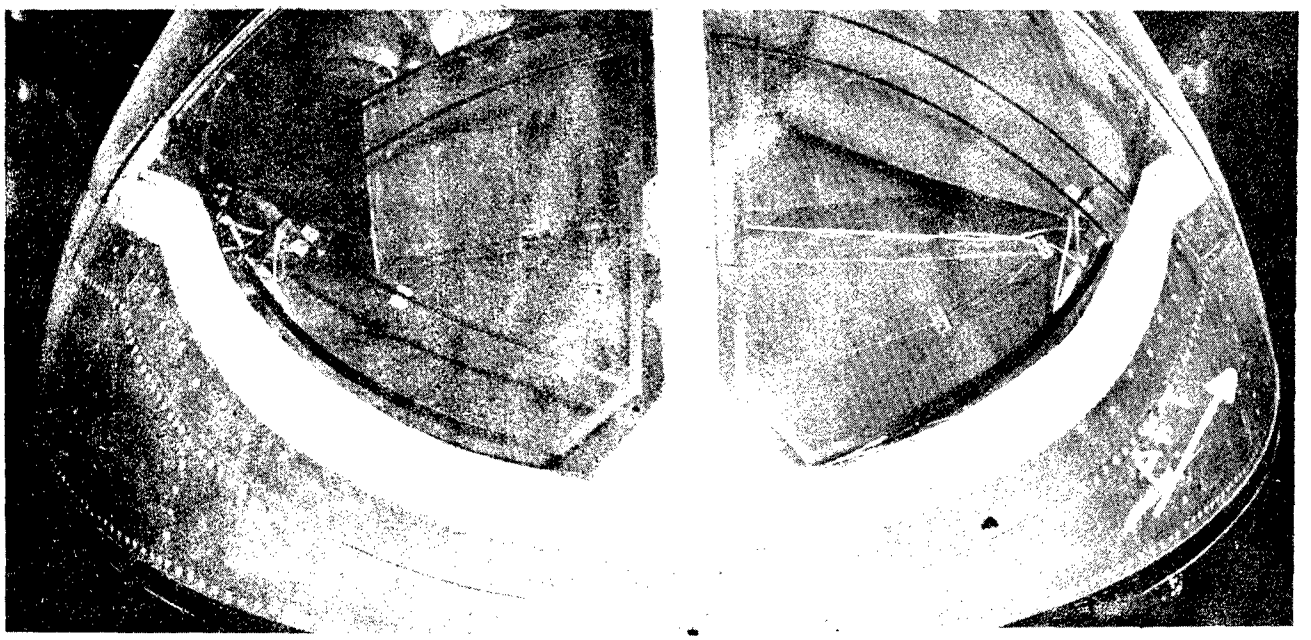

Figure 10
Outside View of Noise Pickup Probes Installed in Nose Canopy

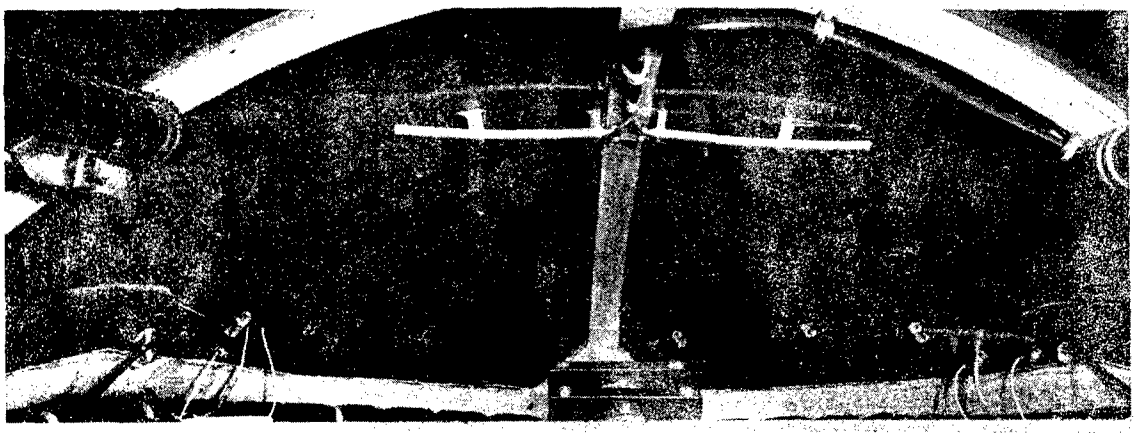

Figure 11
Installation of Noise Pickup Probes in Nose Canopy

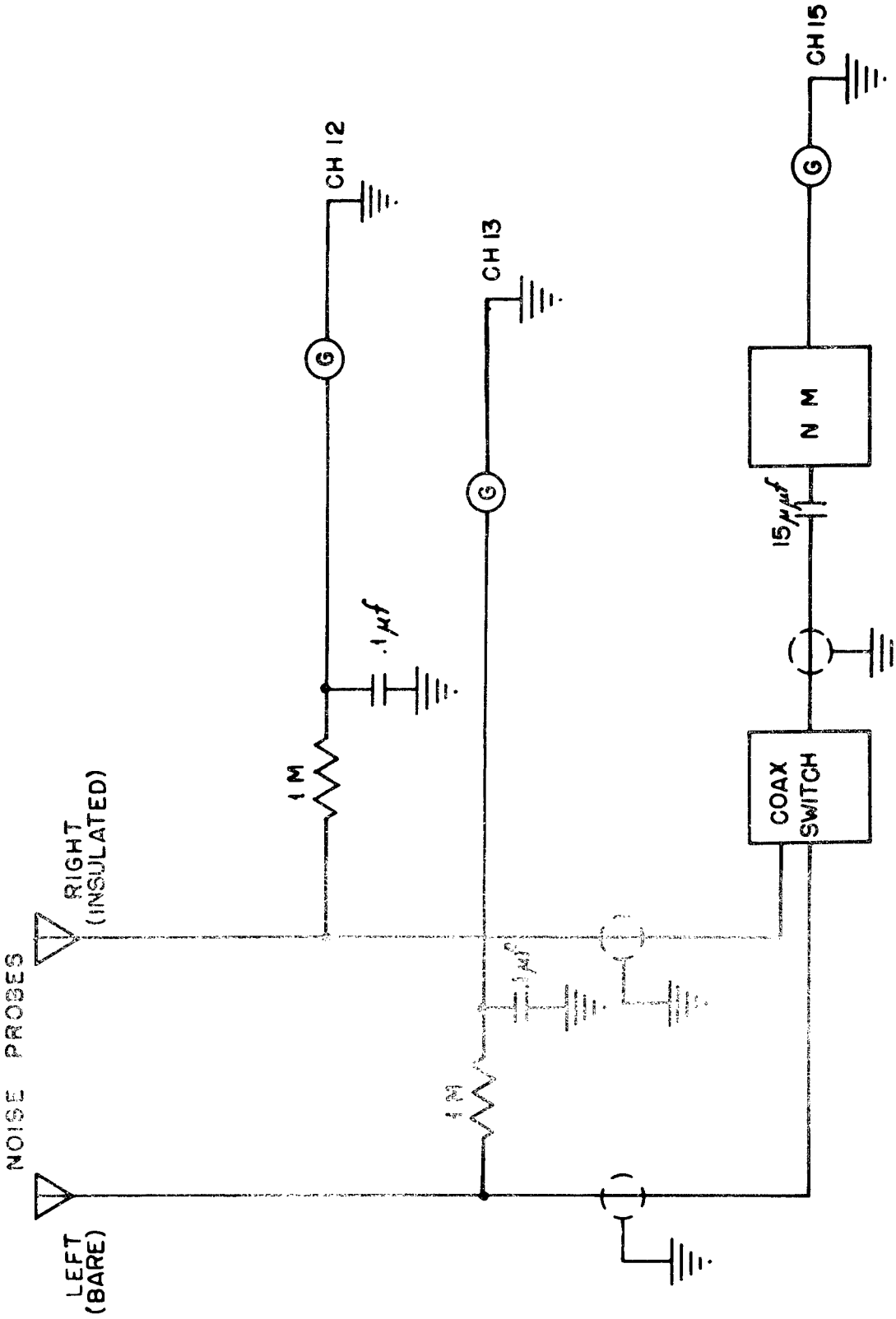

Figure 12
Block Diagram of Noise Meter Installation

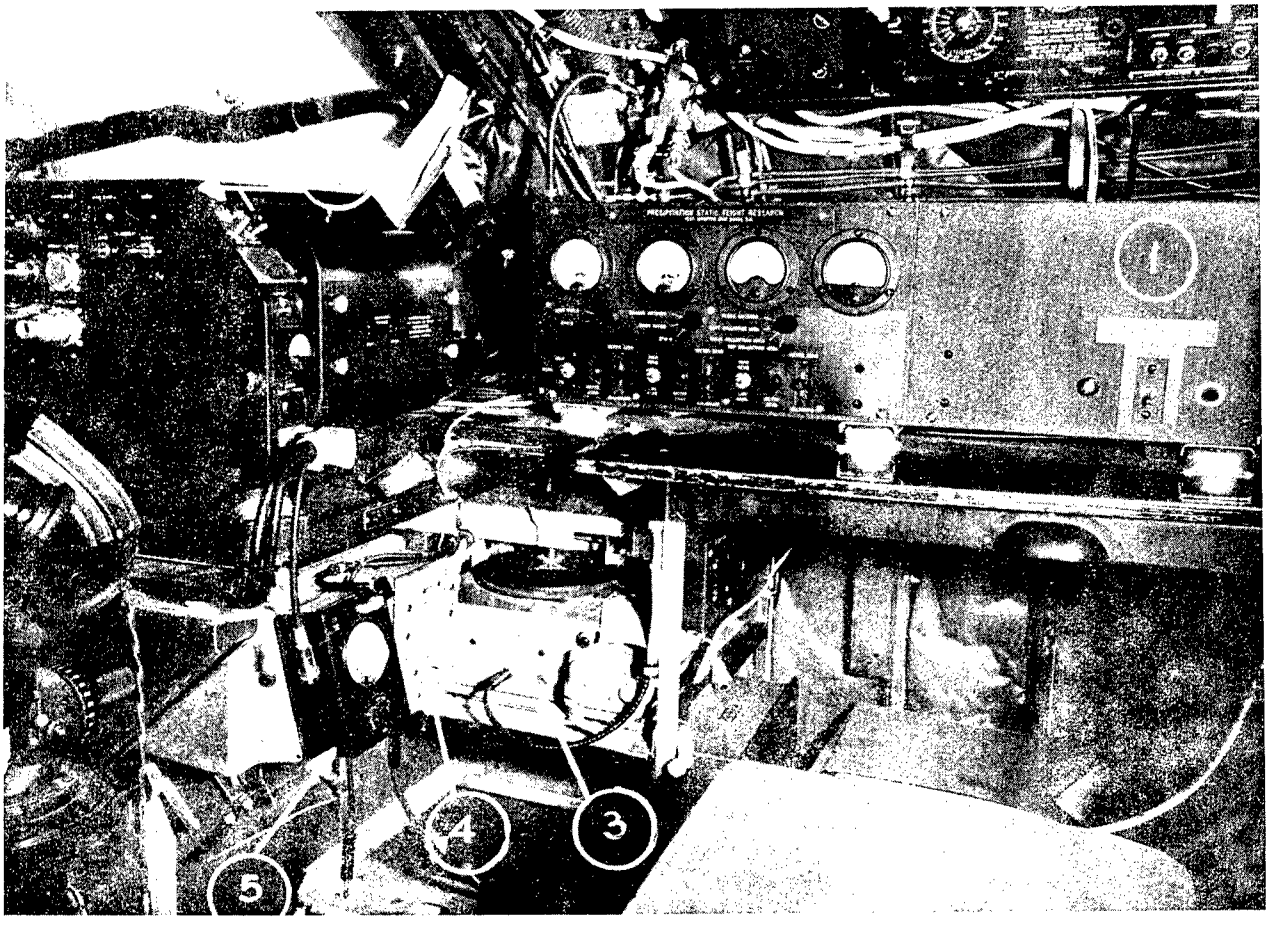

Figure 13
Internal View of Nose of Test Aircraft

Figure 12, page 9, is a block diagram of the noise meter installation. Corona current from each noise probe was monitored on two additional channels of the oscillograph. One probe was insulated to prevent it from going into corona, and the other was left uninsulated. Figure 13, page 10, and Figure 14, page 11, are internal views of the nose of the aircraft, showing the complete instrumentation, including the noise meter. Figure 1 and 12, pages 2 & 9, are block diagrams of the instrumentation showing the function of all components.

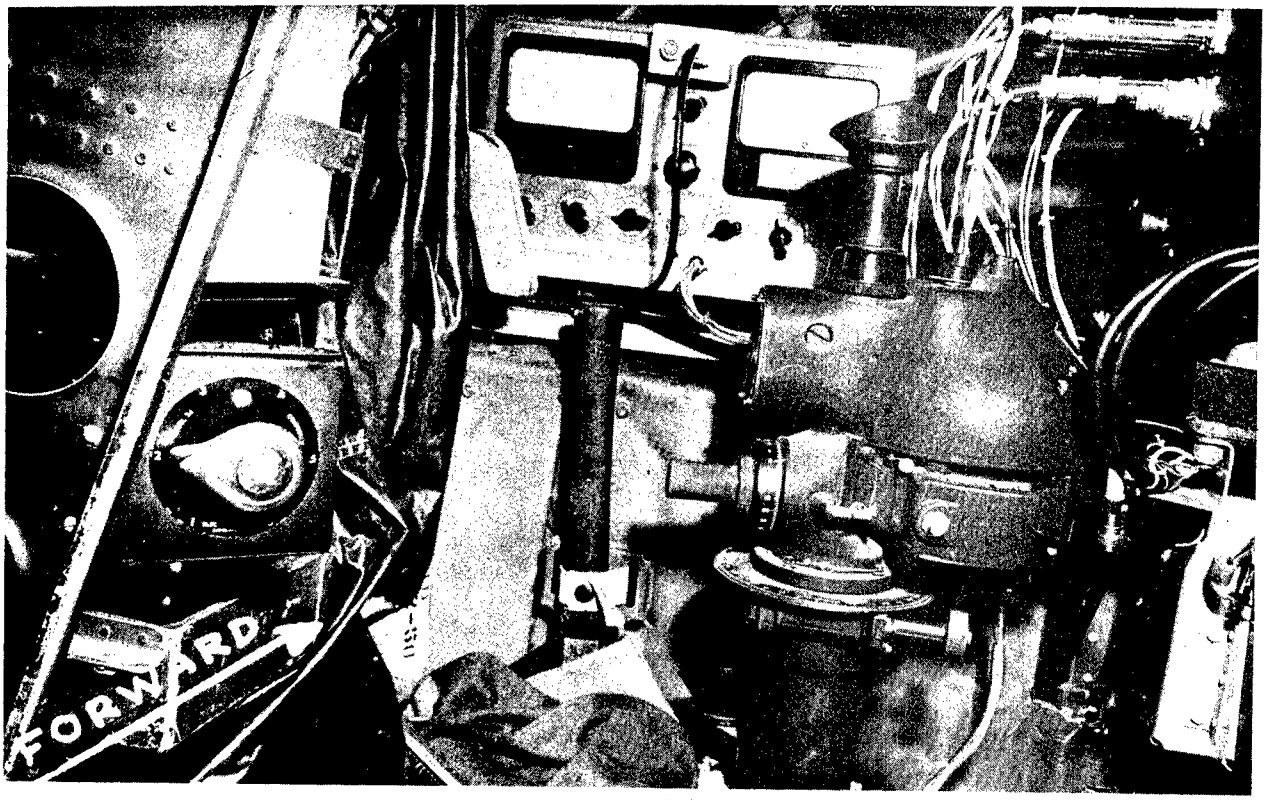

Figure 14
Installation of Special Noise Meter and Associated Equipment in Nose Compartment

The raw data is received on a continuous strip of paper, containing continuous records of all 16 quantities as a function of time. Figure 15, page 12, is a portion of a record of this type. The data is of limited usefulness in this form. The most useful form of the data is a plot on rectangular coordinates of one quantity as a function of another. Figure 16 is a photograph of a data analyzer built for this laboratory by Gaveco Laboratories, Inc. With this data analyzer, any given oscillograph trace is tracked with a light spot as the oscillograph record is slowly moved past the spot. There are two such spots with independent positioning controls, to permit two operators to track two traces simultaneously. The output of the data analyzer, which is two independent voltages proportional to the positions of each light spot, is fed into an X-Y recorder. The combination of the data analyzer, and an X-Y recorder are shown in Figure 17, page 14. The result is a rectangular plot, similar to those in Figure 18 through 36.

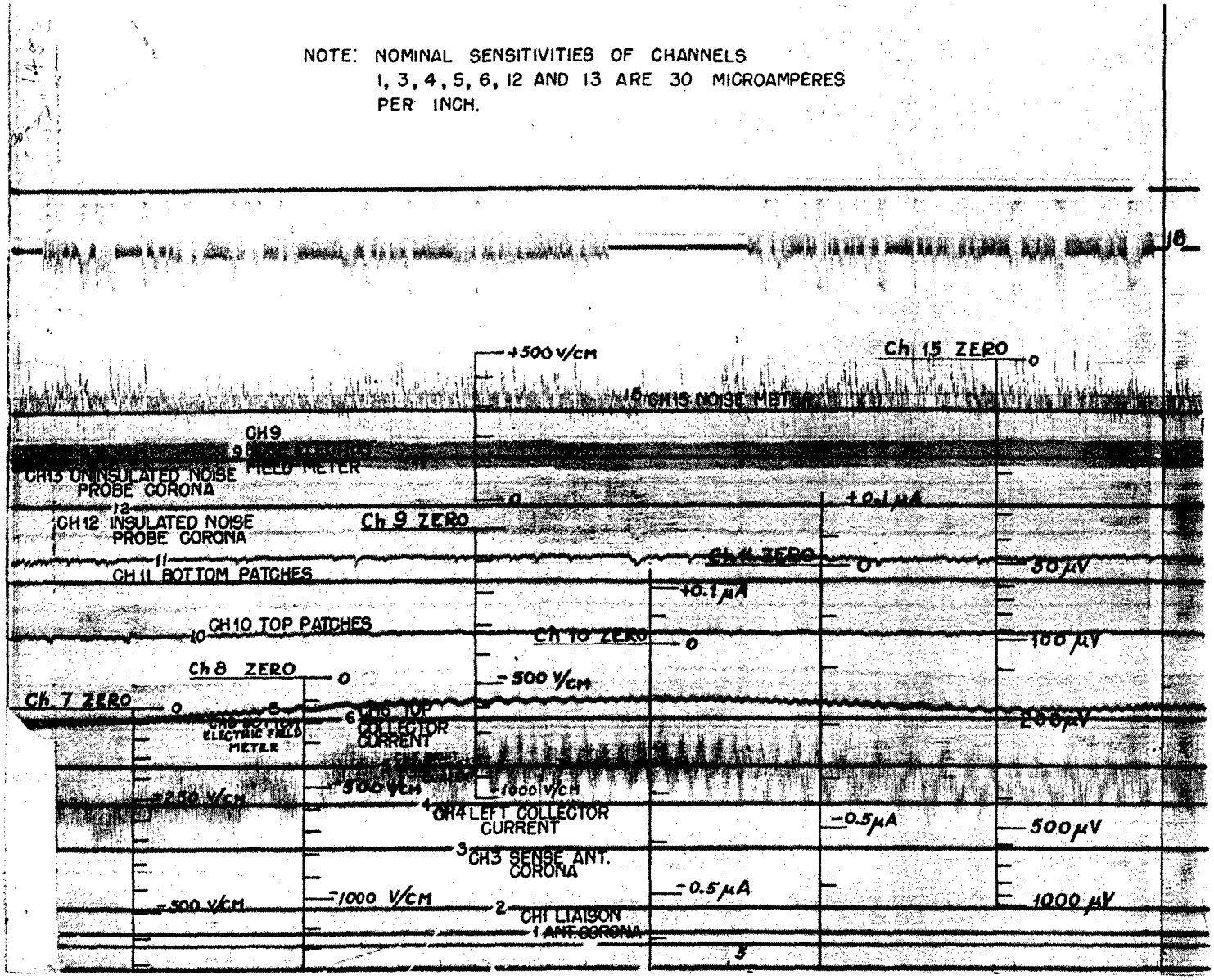

Figure 15

Sample Oscillograph Record

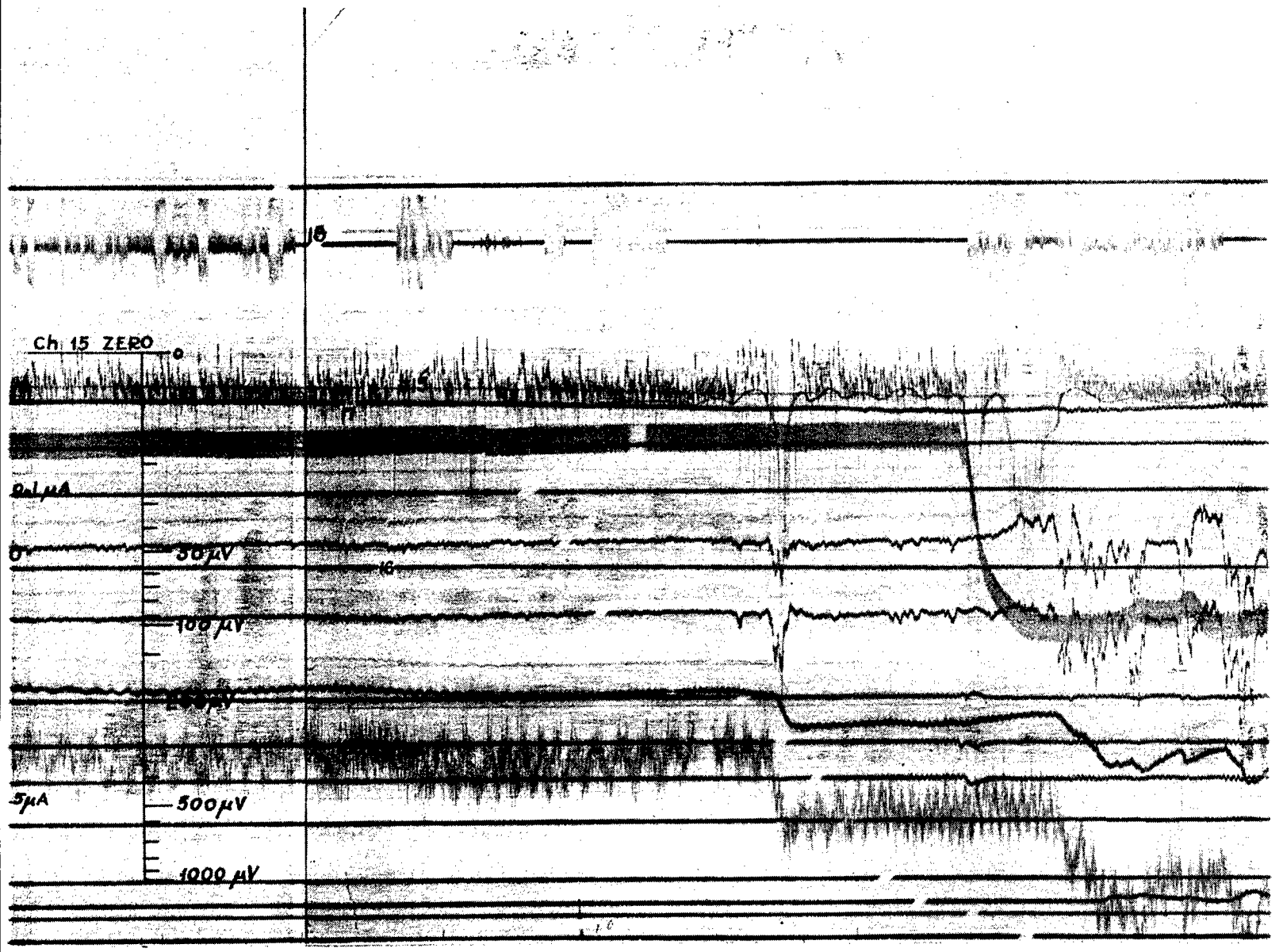
Ch 15 ZERO
0
5
10
15
16
0.1 μA
50 μV
100 μV
5μA
500 μV
1000 μV

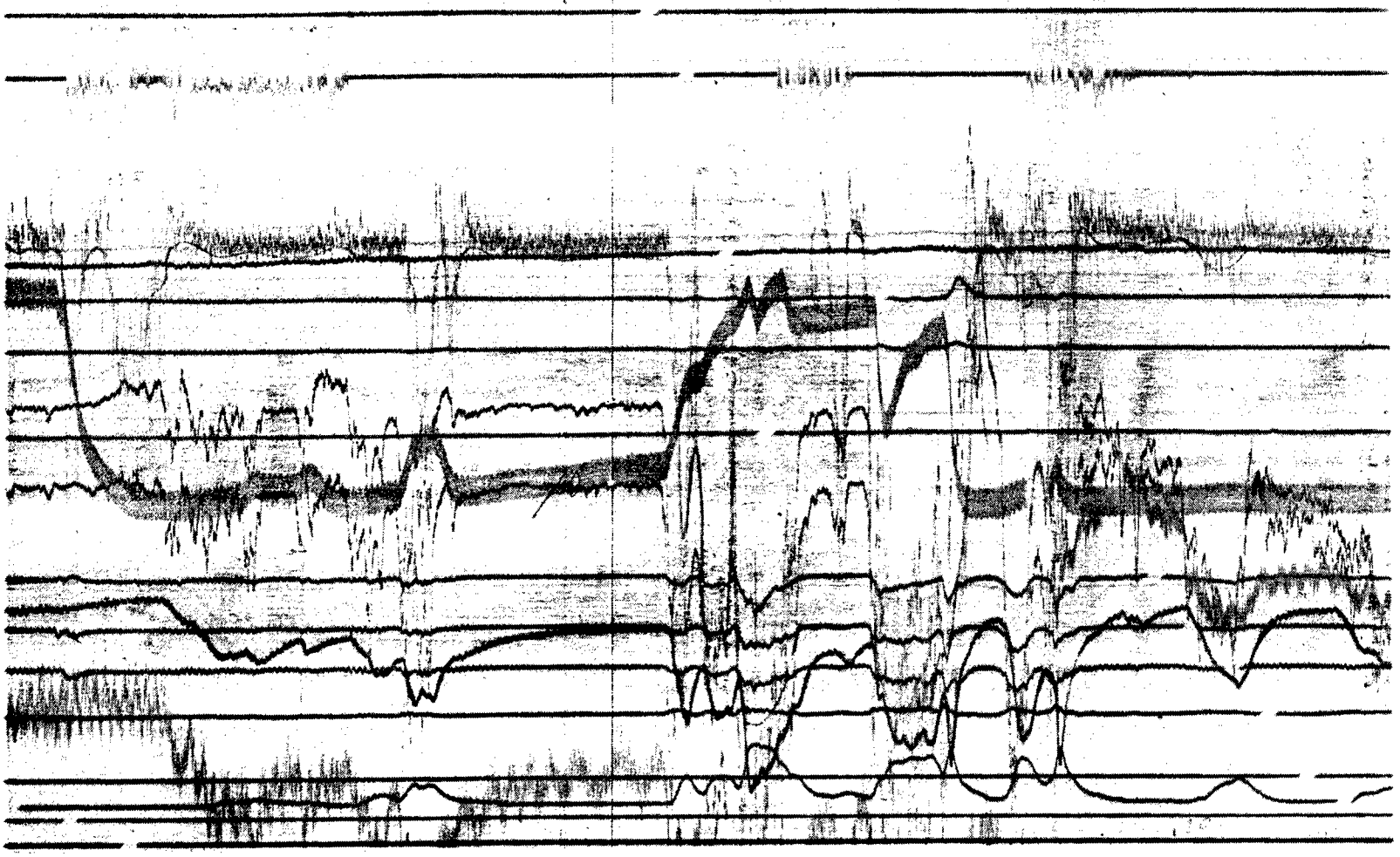

2A

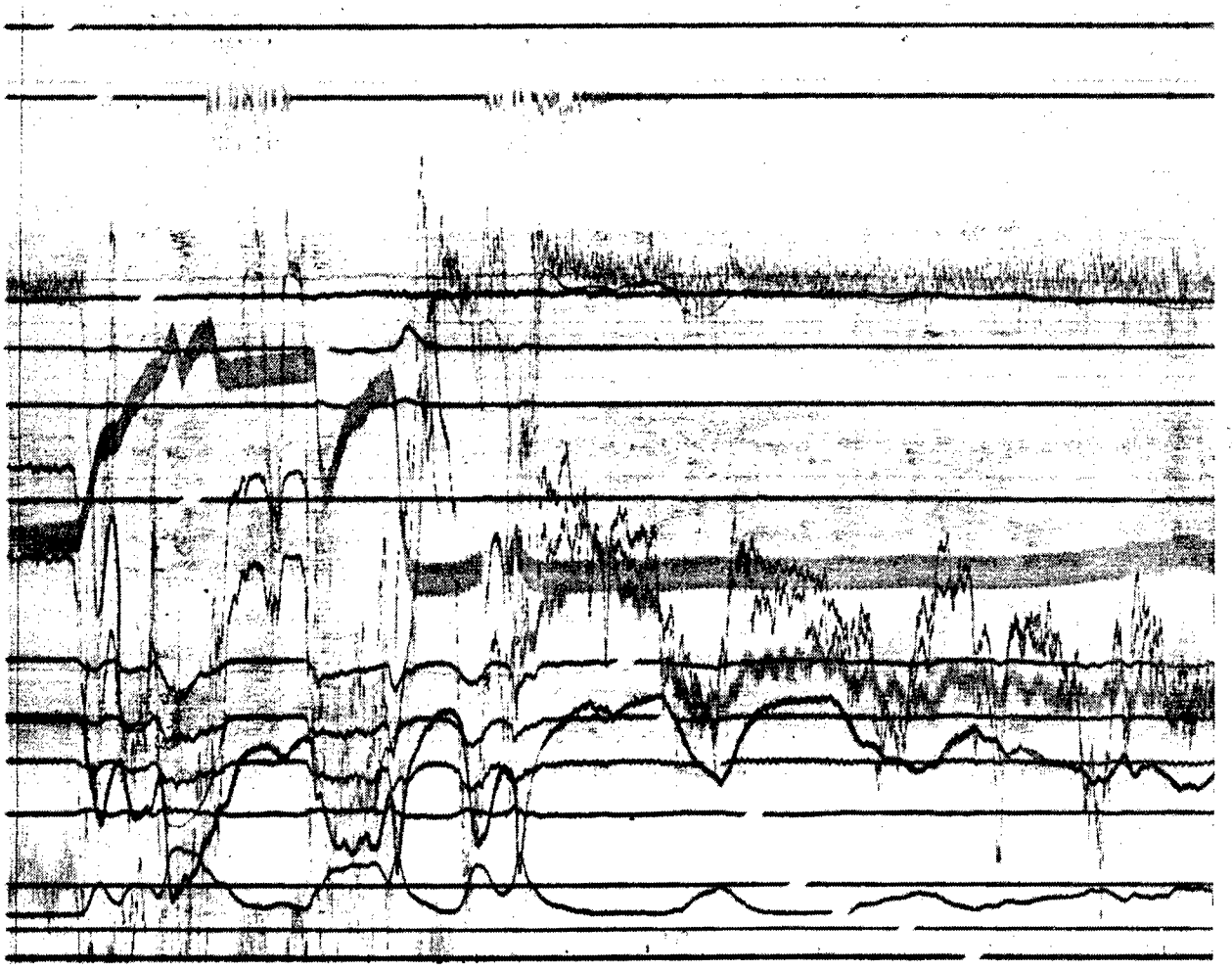

2°

3

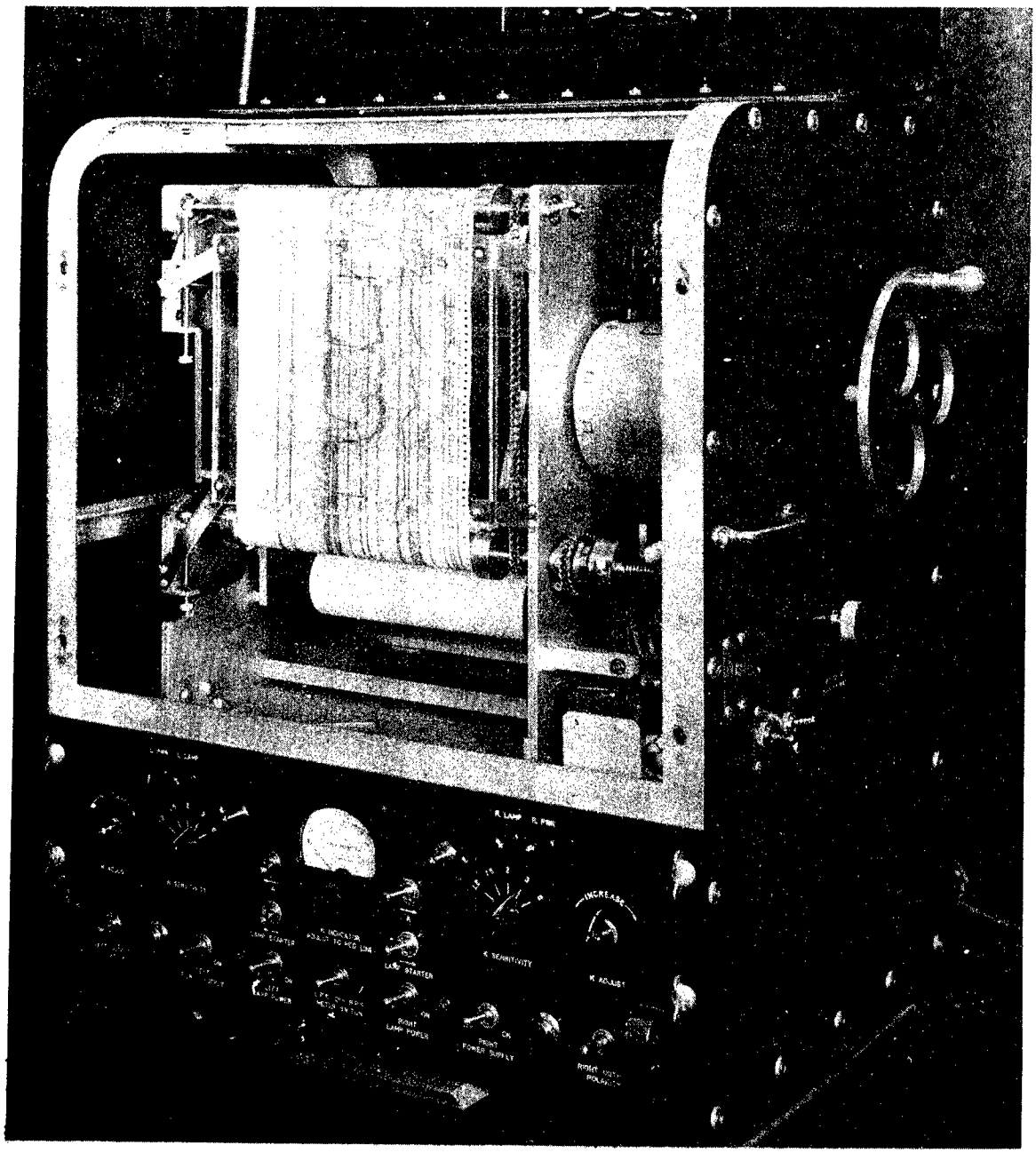

Figure 16
Data Analyzer MX-(XA-123)/U

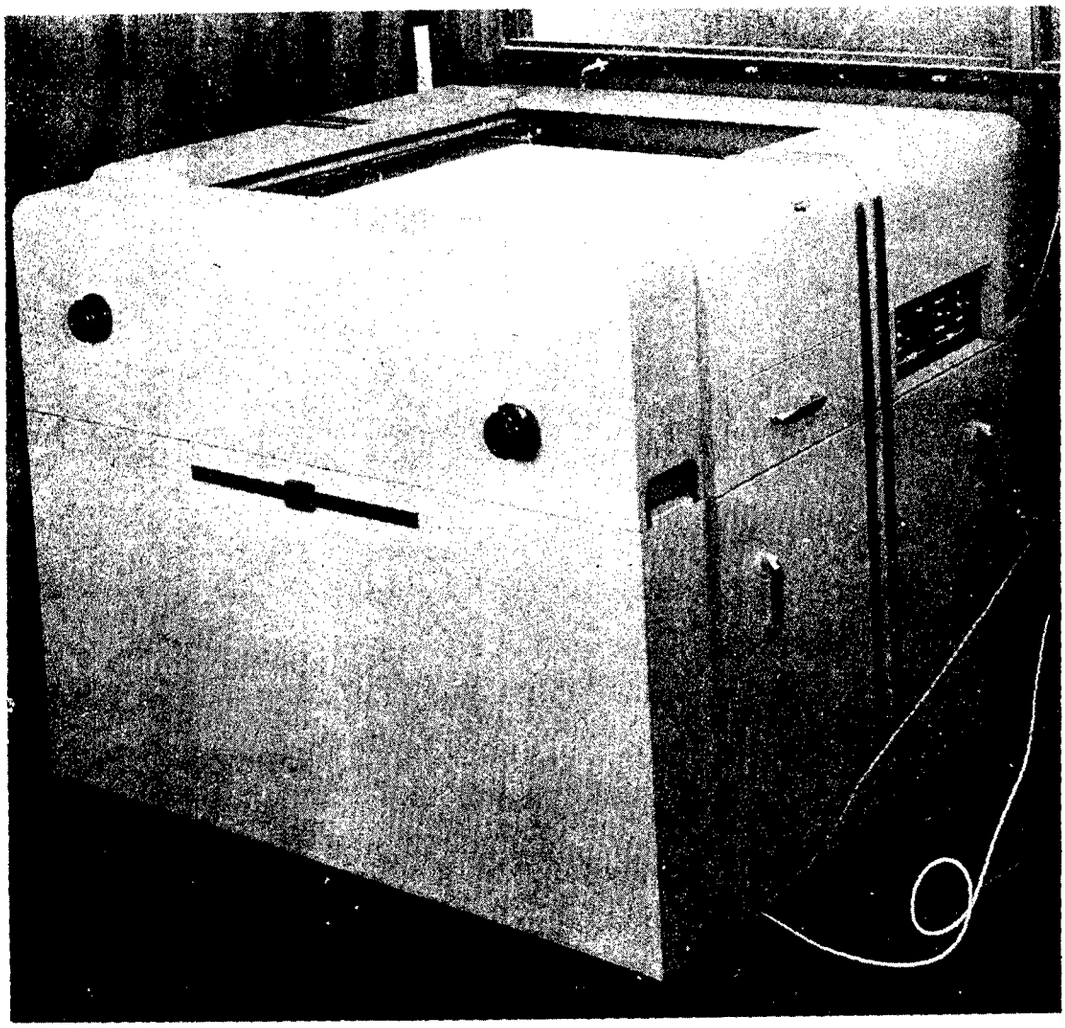

Figure 17
Variplotter (Electronics Associates, Inc., Model 205B) and Data Analyzer MX-(XA-123)/U

SECTION II
TESTS AND TEST RESULTS

Eleven flights were made in the period from 2 October 1950 through 17 March 1951. These flights were made through weather varying from clear air to high level ice crystals at low temperatures. Clear air flights were shakedown flights for the instrumentation, and also were used to calibrate the altitude and indicated air speed traces on the oscillograph. Additional flights were made through precipitation, varying from wet snow and rain at or near the freezing level to ice crystals at temperatures of -20° to -40°C.

A basic piece of information needed to determine the charging characteristics of the aircraft is the manner in which the electrostatic field varies with the charging current. This information was obtained by flying through precipitation of varying density with uniform power settings. Oscillograph records were obtained.

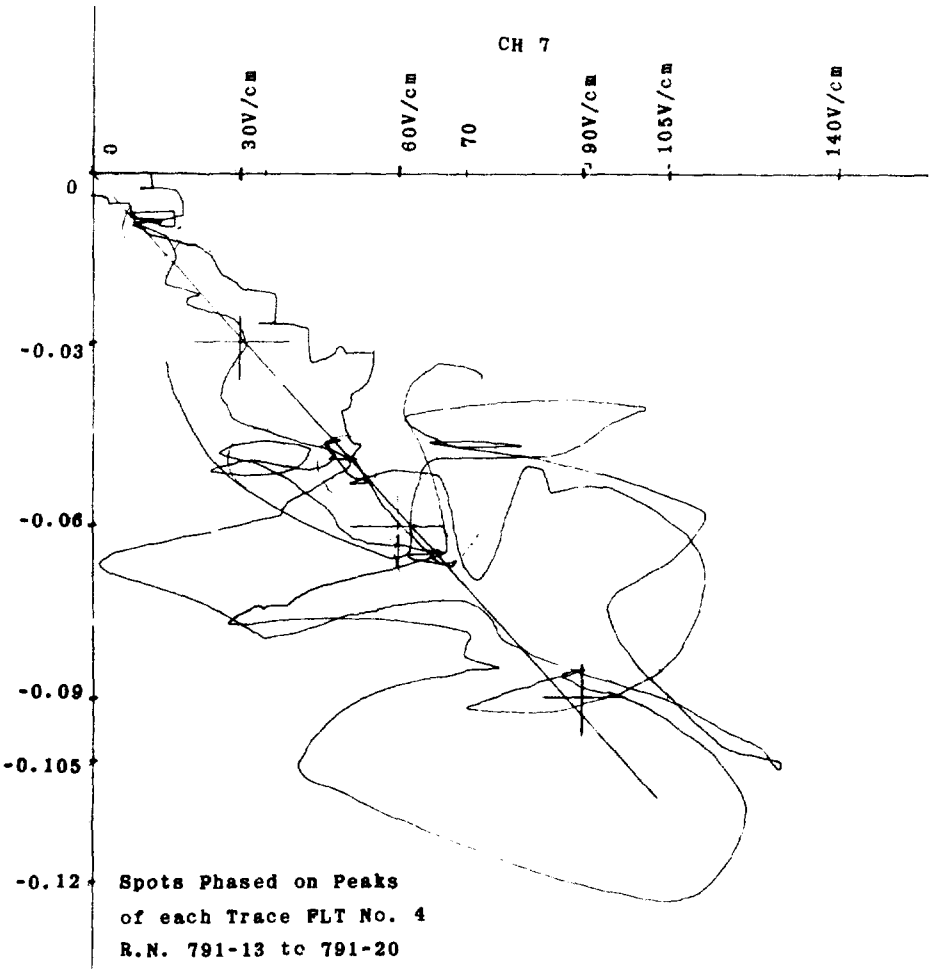

Figure 18
Top Electric Field as a Function of Charging Current

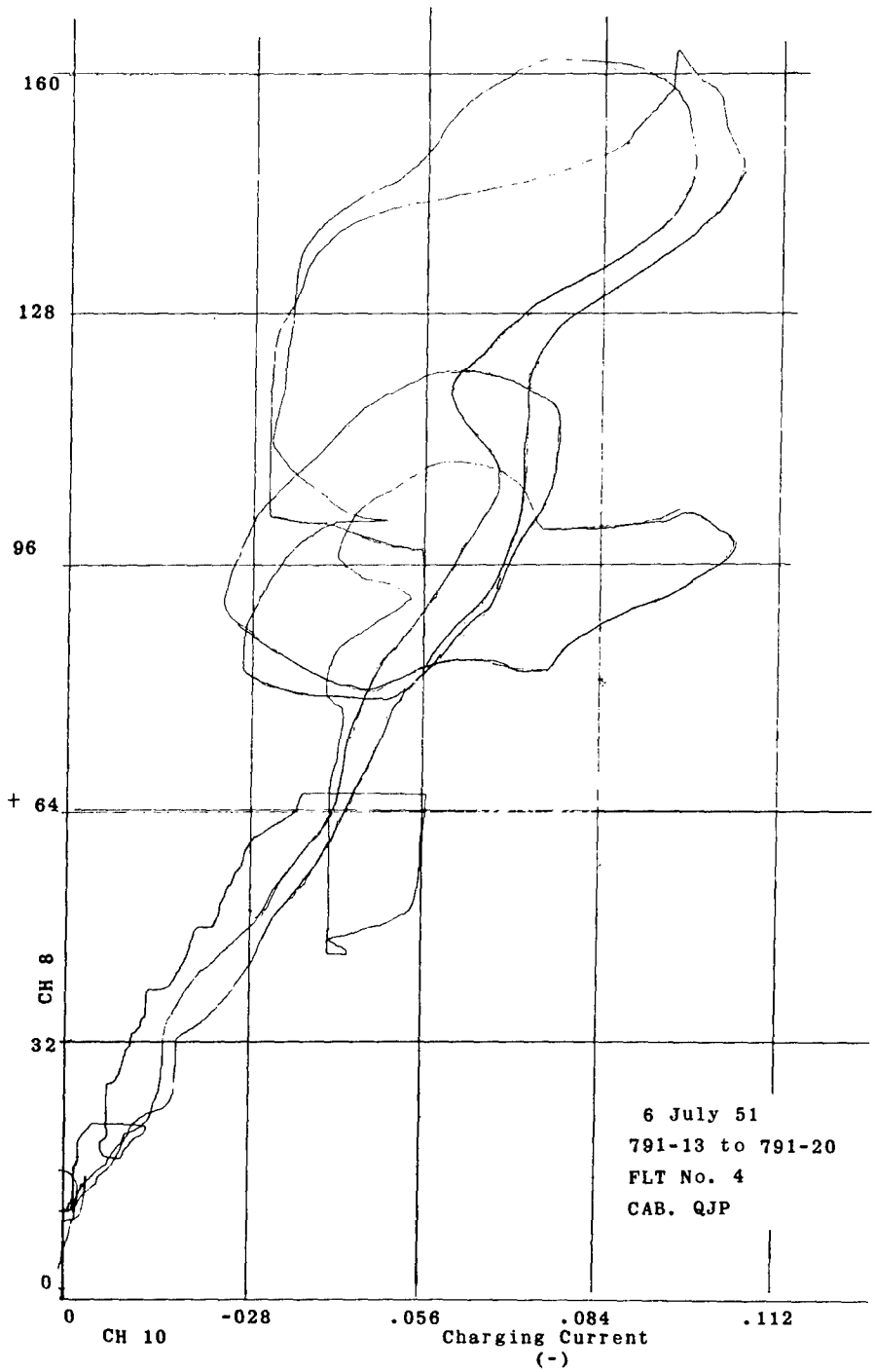

Figure 19
Bottom Electric Field as a Function of Charging Current

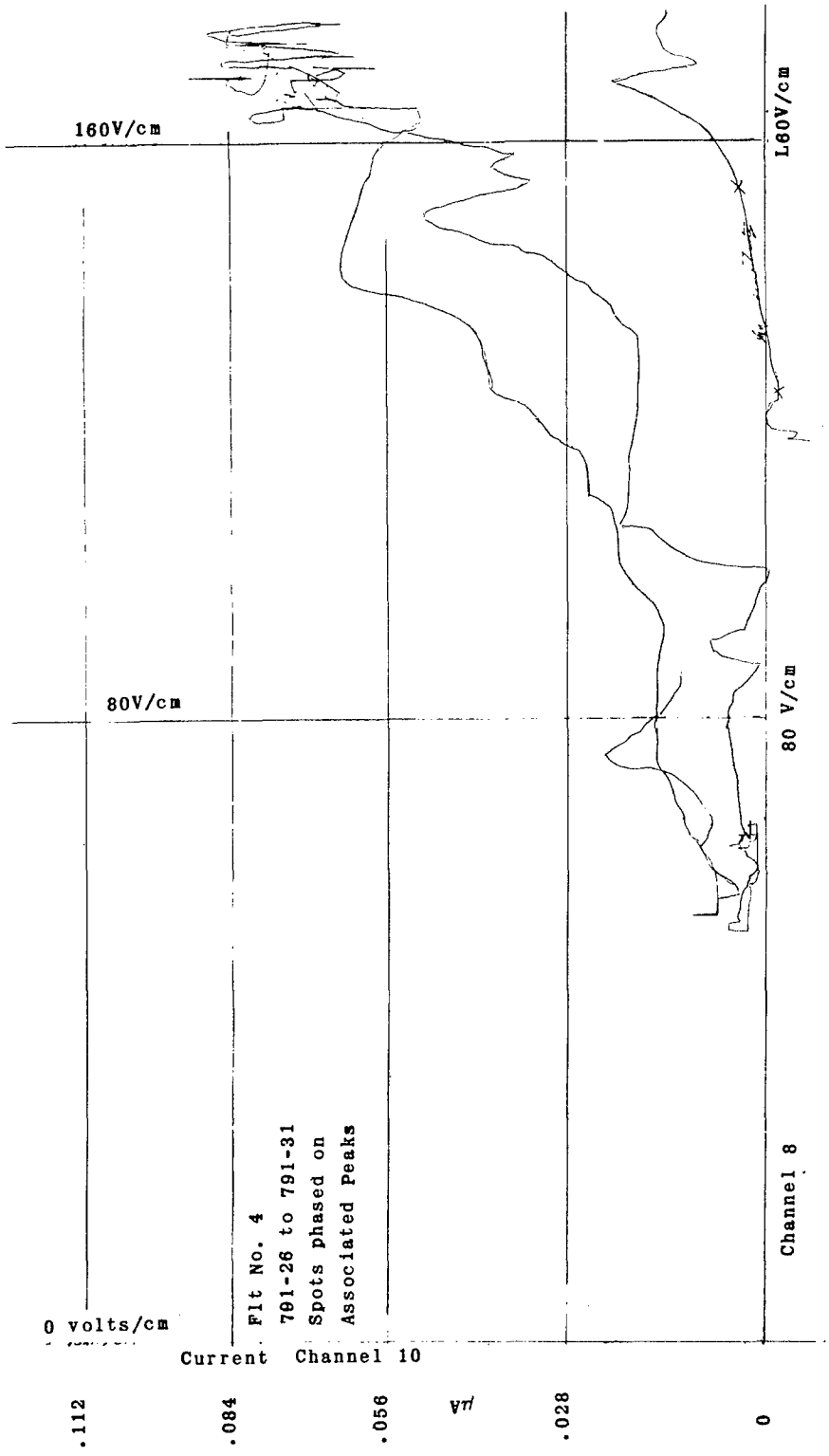

Figure 20
Bottom Electric Field as a Function of Charging Current

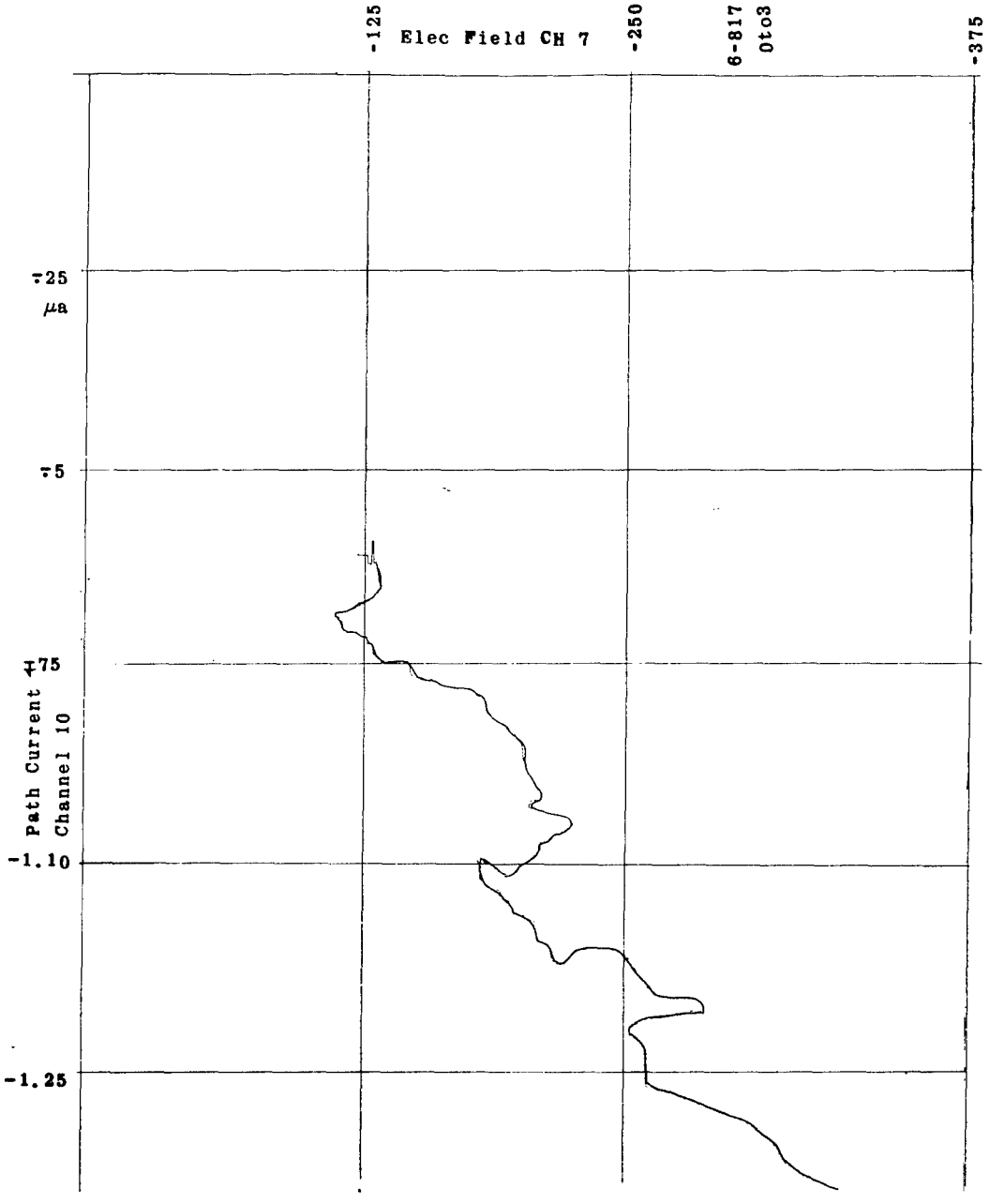

Figure 21
Top Electric Field as a Function of Charging Current

on flight numbers four and six which were suitable for obtaining this data. Figures 18, 19, 20, and 21, pages 15, 16, 17, and 18, respectively, are graphs made with the Data Analyzer of portions of the oscillograph records from flight numbers four and six. It may be seen readily that the relationship between charging current to the metal patches and electric field, for charging currents to the patches less than or equal to one microampere, and bottom electric fields less than or equal to 1,000 volts per cm, is approximately linear. The total charging current to the aircraft is approximately 1,300 times the patch charging current, which gives a total charging current to the airplane of about 1.3 milliamperes to produce an electric field at the bottom electric field meter of 1,000 volts/cm. The multiplier of 1,300 was arrived at as the ratio of the total projected frontal area of the aircraft to the projected frontal area of the patches. The linear relationship between charging current and electric field is to be expected up to the point where discharge mechanisms other than the engine exhausts begin to operate.

Figure 22, page 20, shows the relationship of top electric field on the aircraft as a whole to the charging current to the plastic nose canopy to be approximately linear, up to fields of -380 V/cm and currents of -5 microamperes. Currents to the collector area would be expected to bear some relationship to the electric field on the aircraft, although not necessarily the same relationship the metal patch currents bear to the field. The ratio of canopy collection current to metal patch current, corrected for differences of area, varied from 1.34 at one microampere collector current to 0.48 at six microamperes collector current. The charging currents to the aluminum and Plexiglas were equal at a current of five microamperes to the collector area. This crossover was probably caused by different angles of incidence of the aluminum patches and the collector area, variation of angle of incidence over the collector area, and differences in surface conditions on the two regions.

The expected relationship, based on previous experience with conventional type aircraft, between true air speed and charging current is:

$$I = \alpha_1 (TAS)^3 \qquad (1)$$

Where α_1 is a constant of proportionality. Since electric field is a linear function of charging current for low magnitudes of electric field:

$$E = \alpha_2 (TAS)^3 \qquad (2)$$

α_2 is a constant of proportionality. The effect of the higher conductivity of the jet exhausts should be to reduce the exponent of the true air speed term in equation 2. Figure 23-A, page 21, is a graph of electric field vs indicated air speed. Figure 23-B, page 21, is a replot of Figure 23A on log-log graph paper. Figure 23-B indicates that the exponent is not constant, and that the straight portion of the curve has an exponent of six. It is evident that this portion of the data was not taken during uniform charging conditions, and that additional data of this type are needed.

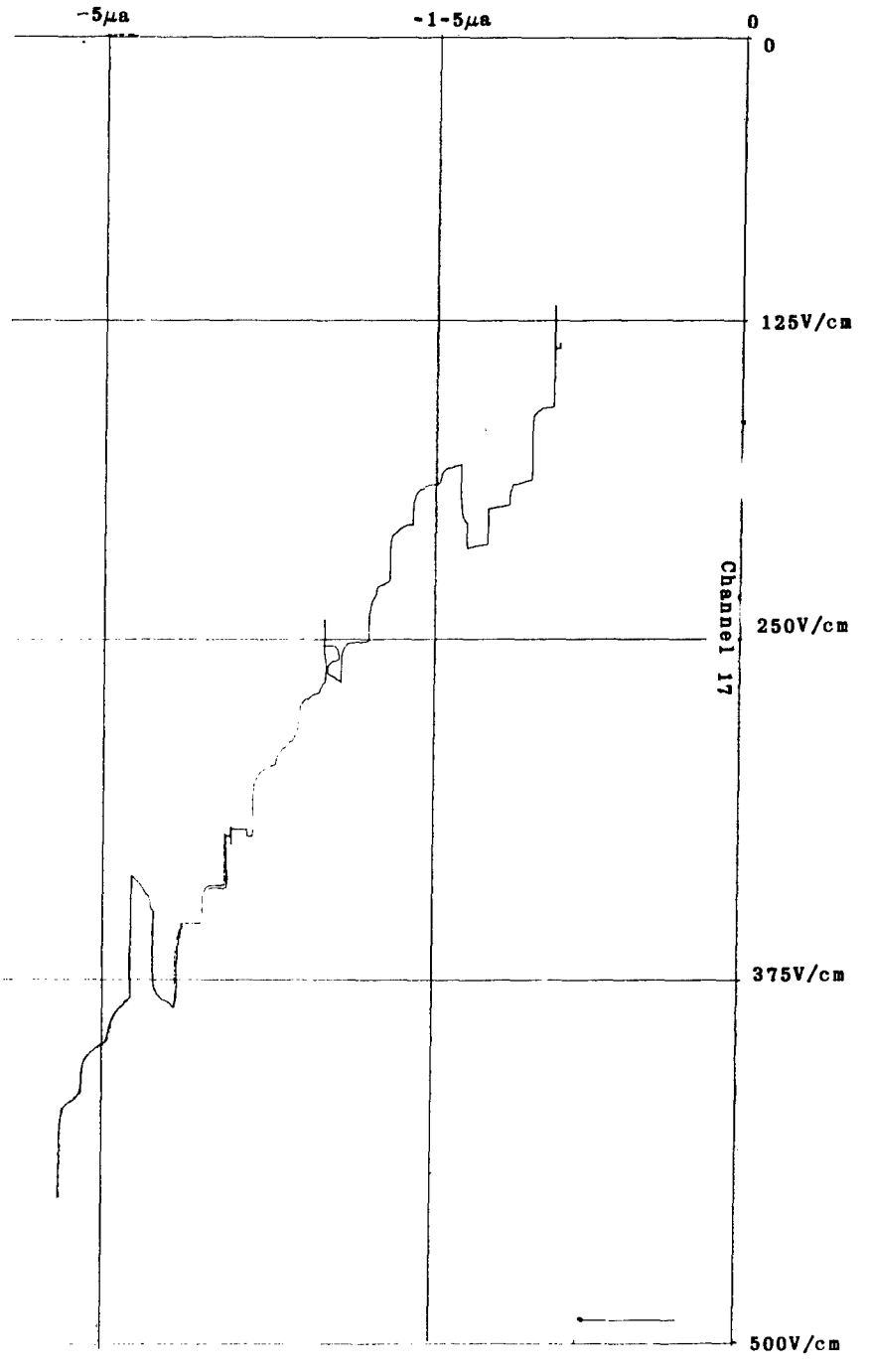

Figure 22
Top Electric Field as a Function of Canopy Charging Current

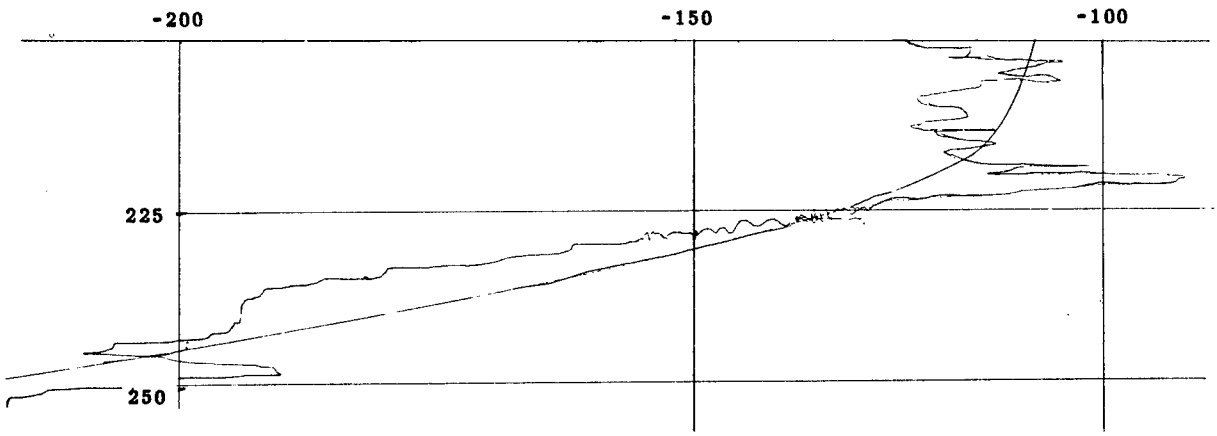

Figure 23A
Top Electric Field as a Function of IAS

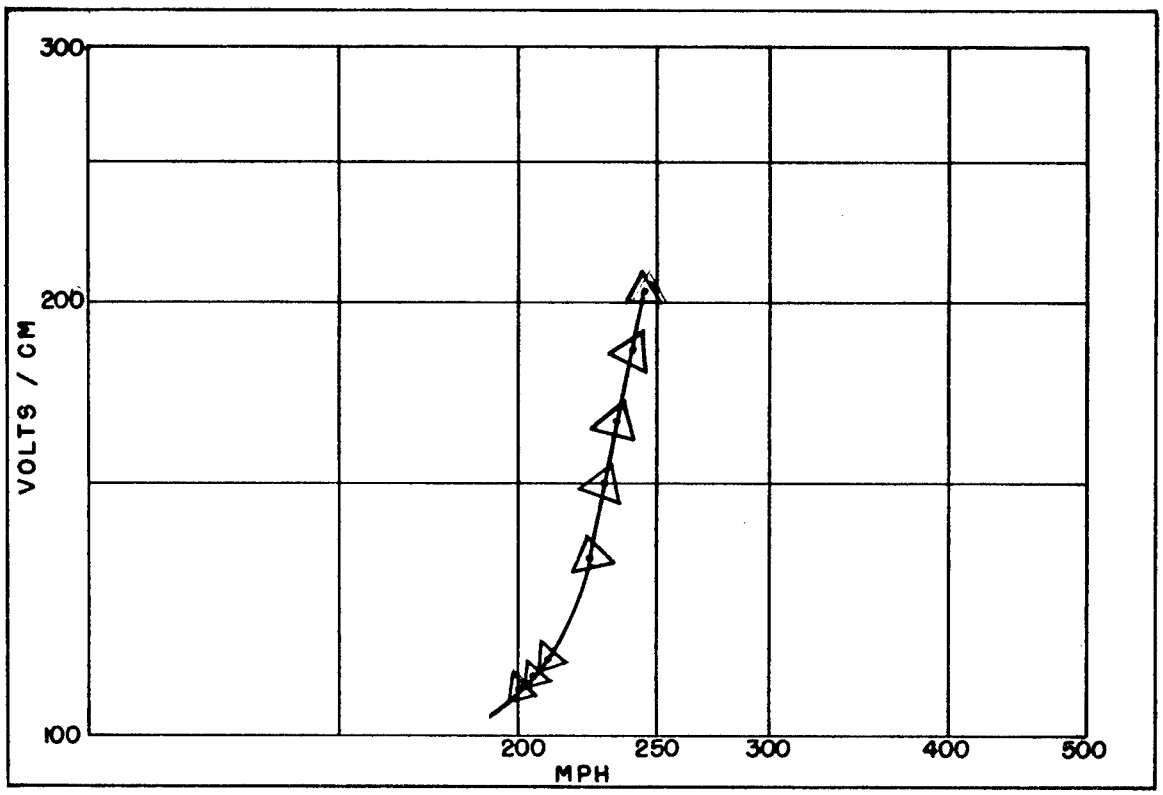

Figure 23B
Top Electric Field as a Function of IAS on Log Log Coordinates

The ratio of the reading of the bottom electric field meter to the reading of the top electric field meter, under pure autogenous charging, should be known in order to make it possible to distinguish between autogenous and exogenous charging. This ratio may be determined from the data of Figures 18, 19, 20, and 21, pages 15, 16, 17, and 18. The ratio of the electric fields for equal charging currents is 1.7, determined from data of Figures 18, 19, 20, and 21. This ratio may be verified by plotting one electric field meter as a function of the other. This has been done, and Figures 24 and 25, pages 23 and 24, show the results. The relationship is linear, and the ratio of bottom to top electric field meters is approximately two. The data for Figures 24 and 25 were taken under widely different conditions, which should give a great deal of validity to the ratio of two.

The B-45 and B-17 type aircraft are similar in size and shape. Previous tests have been made on a B-17 type aircraft, with an antenna placed in a comparable location to the liaison antenna on the B-45. Also, the B-17 had electric field meter detector heads located in similar locations to the ones on the B-45. Thus, there should be an almost direct comparison between the data from the B-17 and from the B-45.

Tests on the B-17 show that the liaison antenna on the B-45 should have a corona threshold in the vicinity of 250 volts/cm, measured on top of the aircraft. Figure 26, page 25, shows that the corona threshold for the liaison antenna on the B-45 was about 500 volts/cm measured on the bottom. If the ratio of two is used for the conversion to top field, we get 250 volts/cm, measured at the top for the corona threshold of the liaison antenna. This is in good agreement with the B-17 data and also gives additional verification to the ratio of two for bottom electric field to top electric field. Figure 26, page 25, shows the discharge characteristic of this antenna is approaching a linear function of the electric field up to 10 microamperes. Previous experience in the high-voltage laboratory, and in flight tests indicate that discharge current from a wire should increase as some rather large exponent of the electric field. This exponent should be at least two, and may go as high as six or more. The discrepancy may be accounted for in the inherent large scatter in the data, and in the limited range of corona currents experienced. The preceding data were taken at a true air speed of 385 mph. The effect of air speed on the exponent of the electric field is unknown, particularly at true air speeds above 300 mph.

Figure 27, page 26, shows the relationship between the nose electric field meter and left front collector current. The positive sign indicates a positive charge at the detector head, indicating a negative charge on the nose canopy. Data of this type are difficult to obtain, since charging currents too minute to measure with the present instrumentation would charge the canopy to high values of electric field, and this charge would remain on the canopy, often until the aircraft was on the ground. A significant relationship would be the nose electric field as a function of the charge on the canopy. The charge on the canopy should be proportional to the charging current to the collection area, multiplied by the duration of the current. The constant of proportionality includes a factor to extend the data obtained from the collection area to the entire canopy.

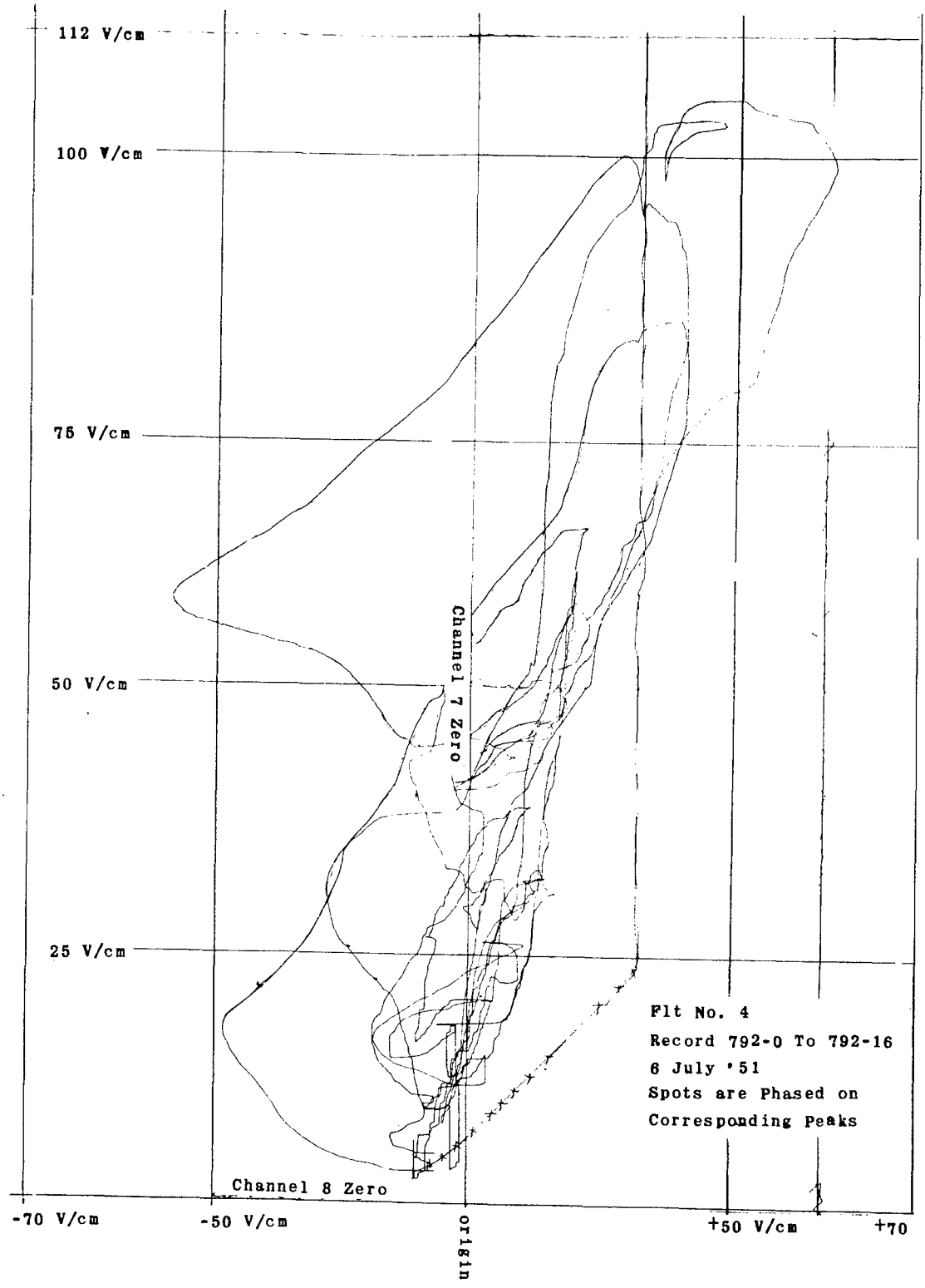

Figure 24 Top Electric Field as a Function of Bottom Electric Field

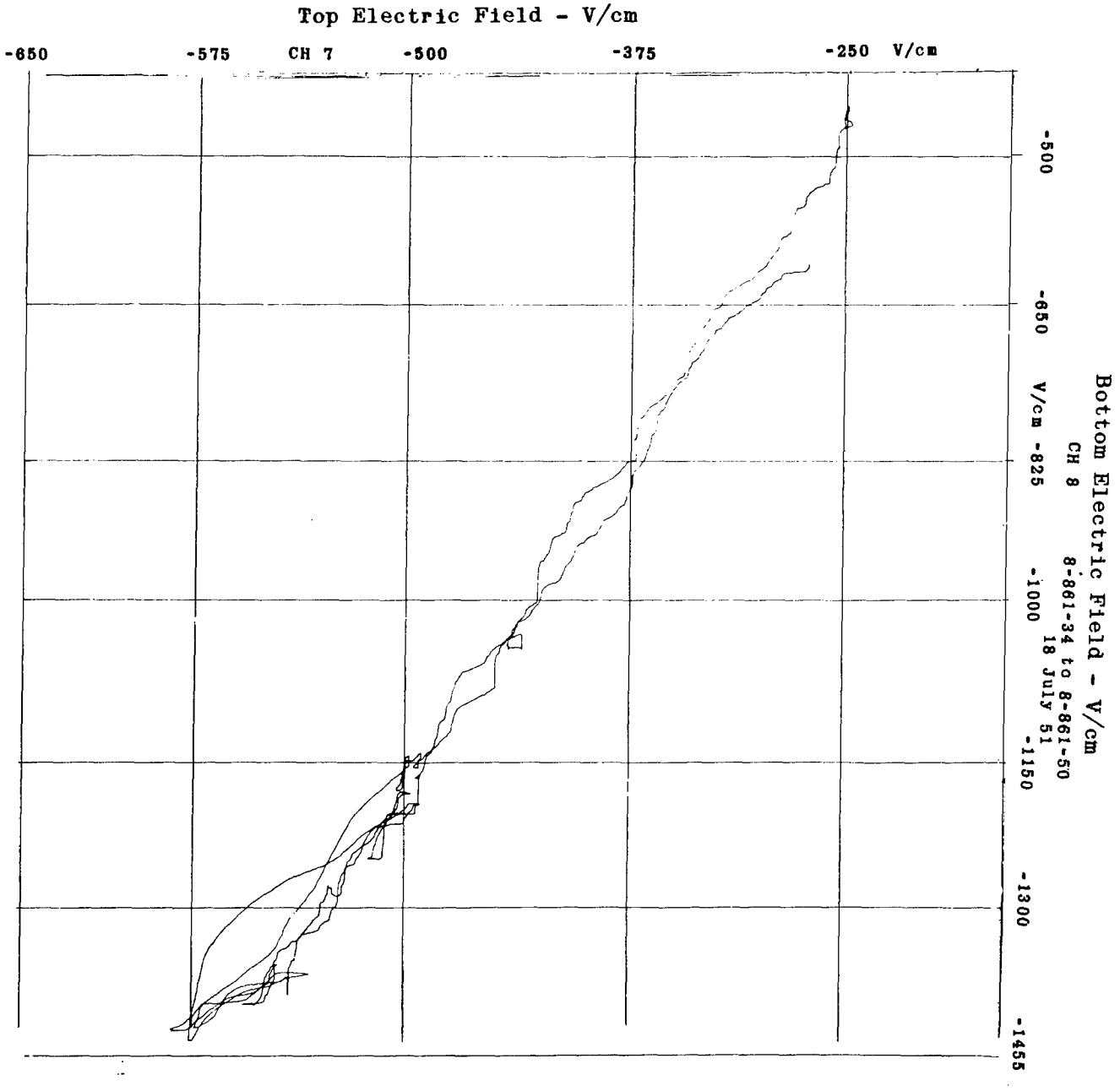

Figure 25
Top Electric Field as a Function of Bottom Electric Field

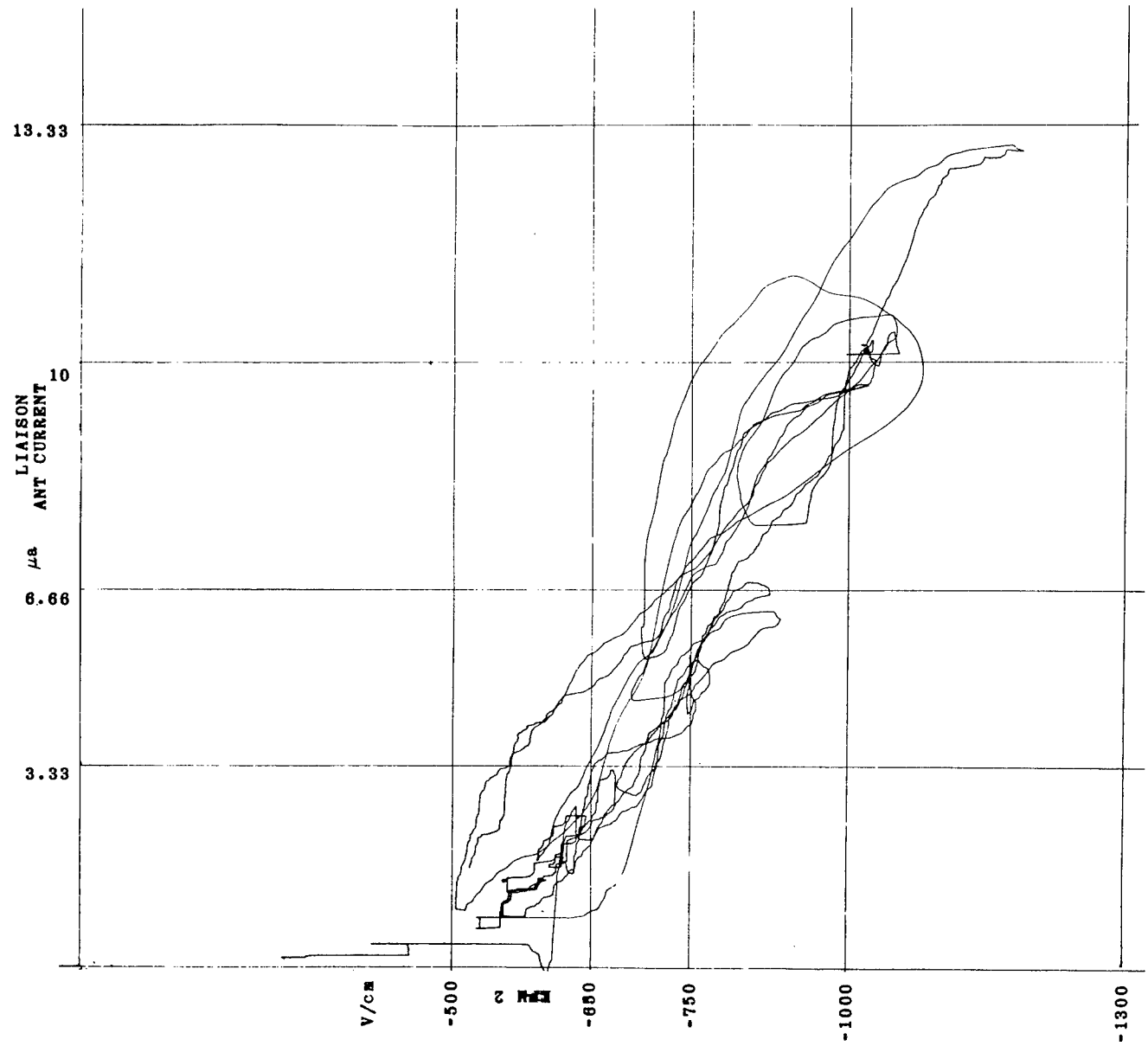

Figure 26
Liaison Antenna Corona Current as a Function of Bottom Electric Field

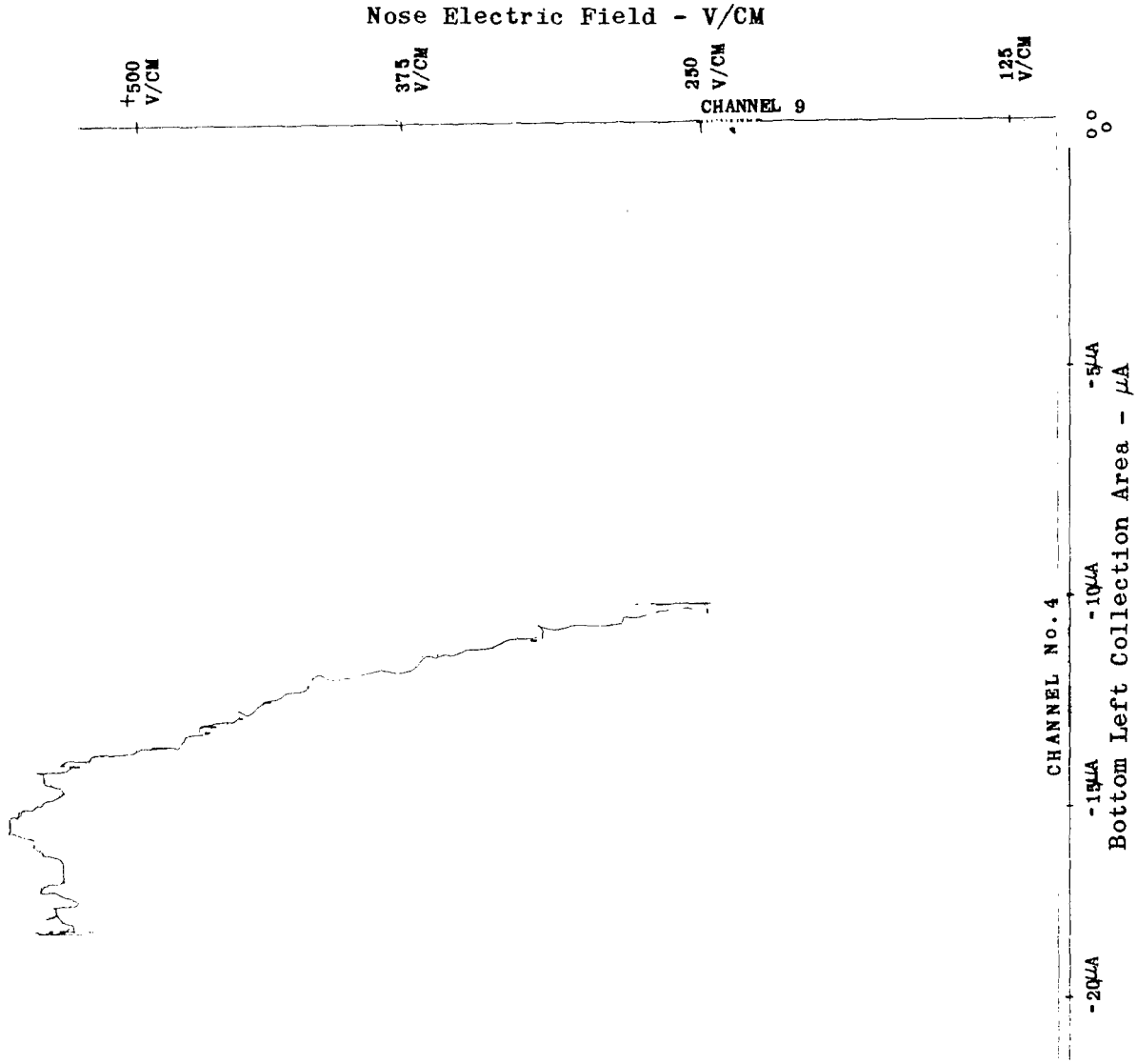

Figure 27
Nose Electric Field as a Function of Canopy Charging Current

Figure 28 is a plot of the nose electric field as a function of the charging current-time product. In the preceding paragraph, mention was made of electric charge remaining on the canopy for relatively long periods of time. This shows that the canopy is a good insulator. Electric field, caused by charge on the canopy, should increase linearly with the quantity of charge on the canopy, assuming no leakage. The gradient across the surface of the canopy then may easily become high enough for localized electrical breakdown to occur across the surface of the canopy. This streamering across the surface offers a satisfactory explanation for the nonlinearity of the curve of Figure 28. Streamering would also account for the decrease in electric field with an increase in the charging current-time product. This streamering is believed to be the source of radio-frequency noise coupled into receiving antennas placed under the canopy.

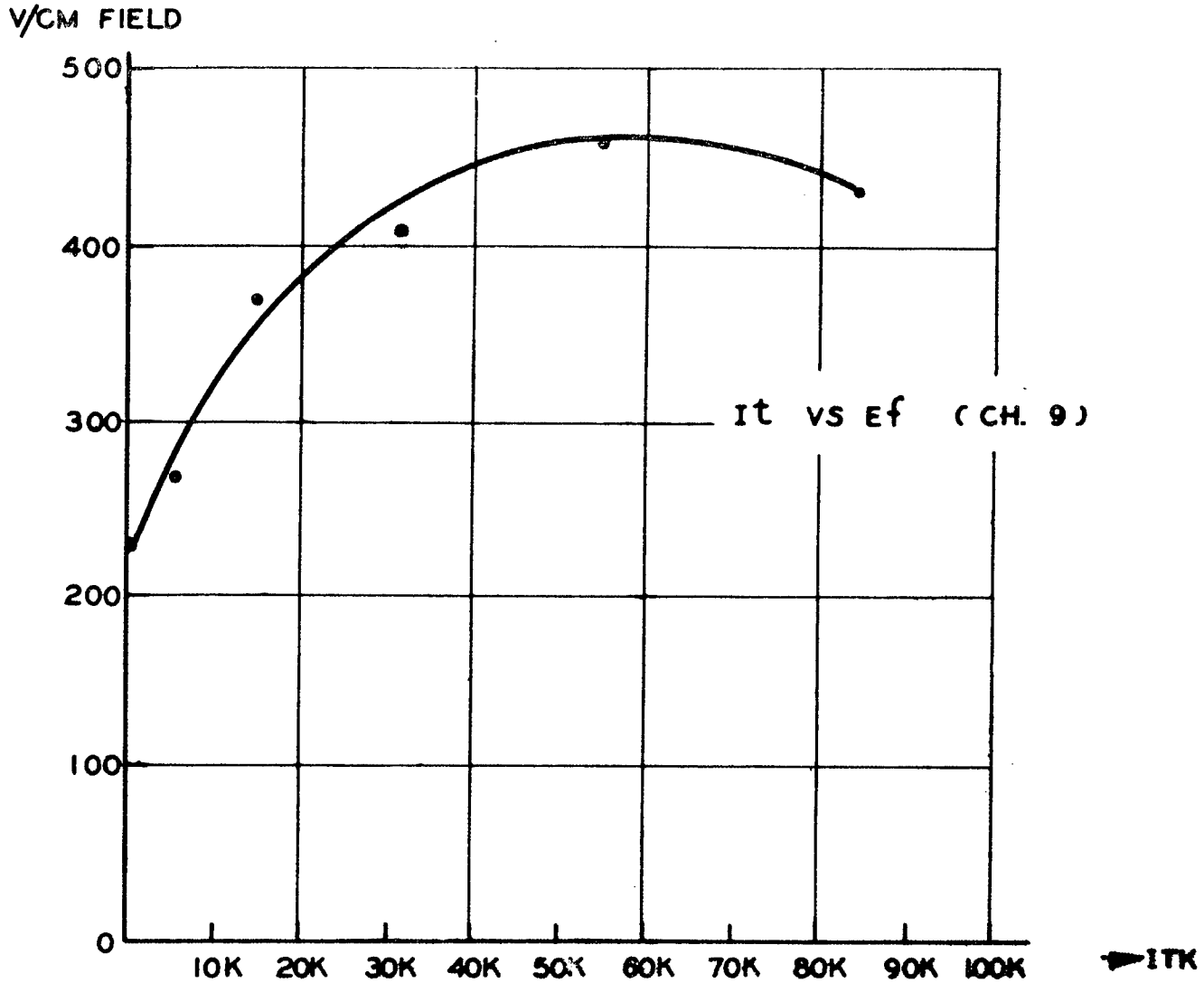

Figure 28
Nose Electric Field as a Function of Canopy Charging Current-Time Product

The relationship of nose electric field to indicated air speed is seen in Figure 29 to be approximately linear. A more significant relationship would be canopy charging current as a function of indicated air speed. Graphs of each collector current as a function of indicated air speed are shown in Figure 30 and 31, page 29, taken on two different flights. The large difference in magnitude is undoubtedly due to a difference in precipitation, and no particular significance should be attached to that difference. However, the graphs give some limited information about the variation of charging current with indicated air speed,

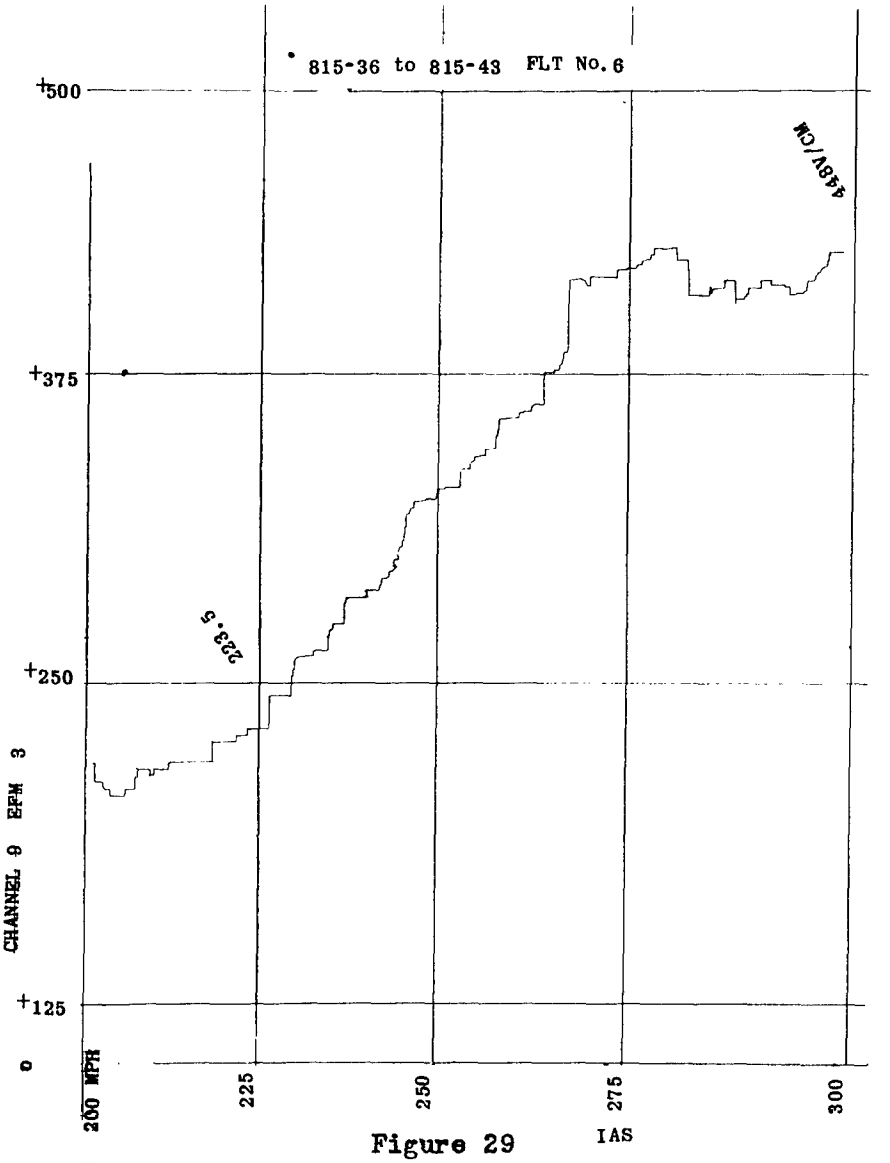

Figure 29
Nose Electric Field as a Function of IAS

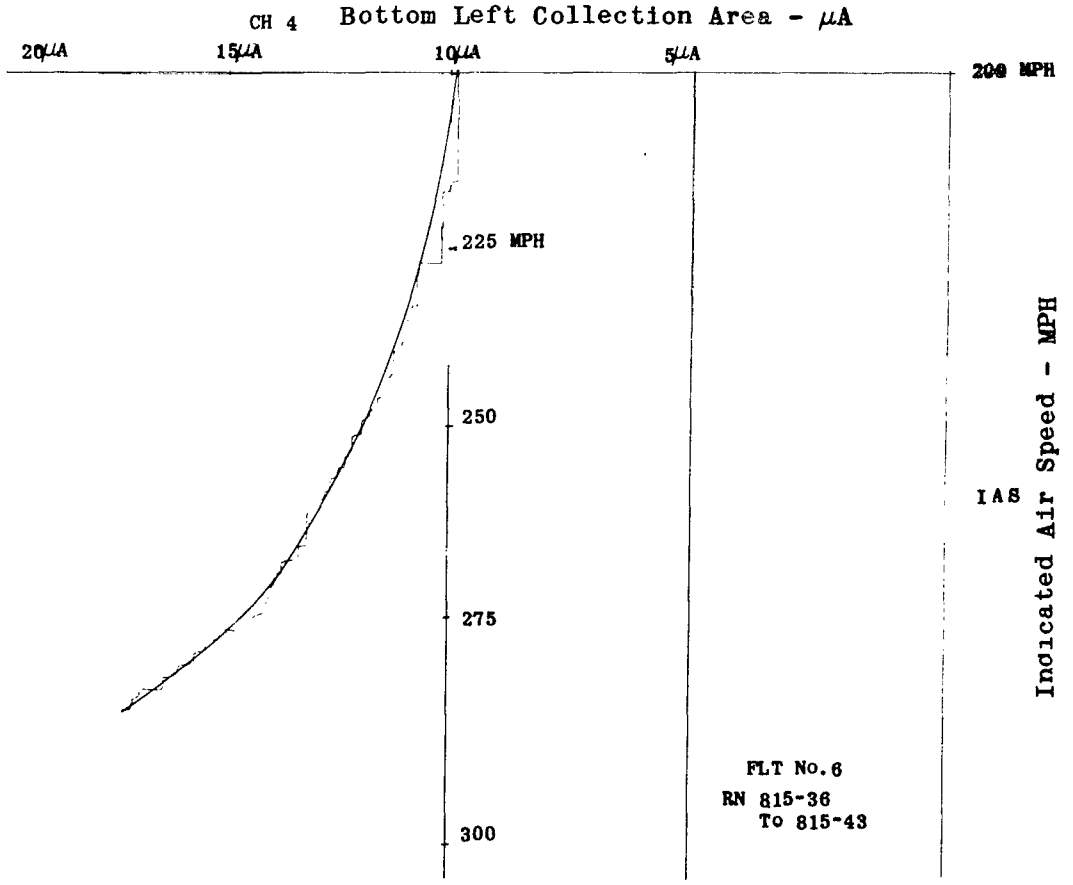

Figure 30
Canopy Charging Current as a Function of IAS

which in the case of Figure 31, page 30, appears to be linear. This agrees with the data of Figure 29 for small currents and fields. However, Figure 30, shows the relationship of the left collector area current to indicated air speed over three times the range of magnitudes of collector currents used in Figure 31. The more extensive data is represented by the following empirical equation:

$$I = 0.011 \ (IAS)^{1.38} \qquad (3)$$

Good data on the relationship of the right front to left front collector currents were obtained on flights six and eight. Equations empirically determined from Figures 32, 33, and 34, pages 31, 32, and 33, are respectively:

Right Collector current = 1.1 Left collector current plus 1.7 (4)

Right Collector current = Left collector current plus 1 (5)

Right Collector current = 1.33 Left collector current (6)

All currents in the above equations are in microamperes. A check was made at a different part of the data from flight six than the above data was taken from. It revealed that for currents greater than 1.5 microamperes, the currents to the right and left front collector areas were equal. However, at currents below this value, the right collector had a greater current than the left collector, and even showed a current of one microampere when the left collector had no current. It is evident that the right collector area has a characteristically higher charging rate than the left collector area. The reason for this condition is impossible to determine exactly with our existing facilities. However, the right collector area is 4.75% larger than the left collection area, and there undoubltedly are differences in the surface conditions on the canopy, which can markedly alter the charging characteristics.

The aircraft used JP-1 fuel up to and including flight 4. After flight four, and before flight five, the aircraft was modified to use JP-3 fuel. Some charging of the aircraft was observed on the first four flights which was attributed to charging by the engine exhausts. The maximum fields observed which were caused by engine exhausts are shown in Table I, Page 33.

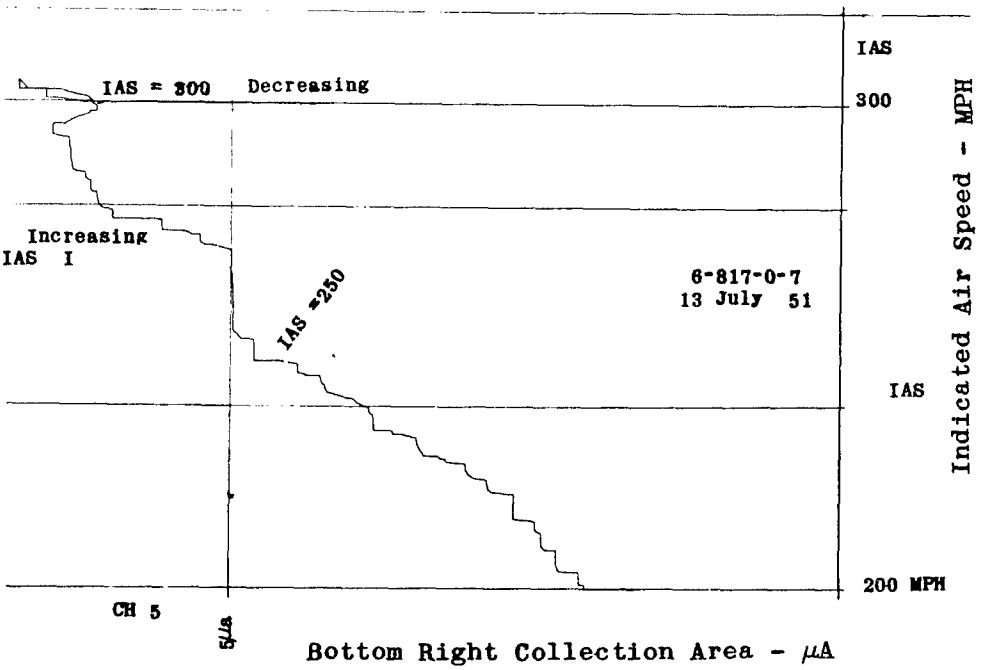

Figure 31
Canopy Charging Current as a Function of IAS

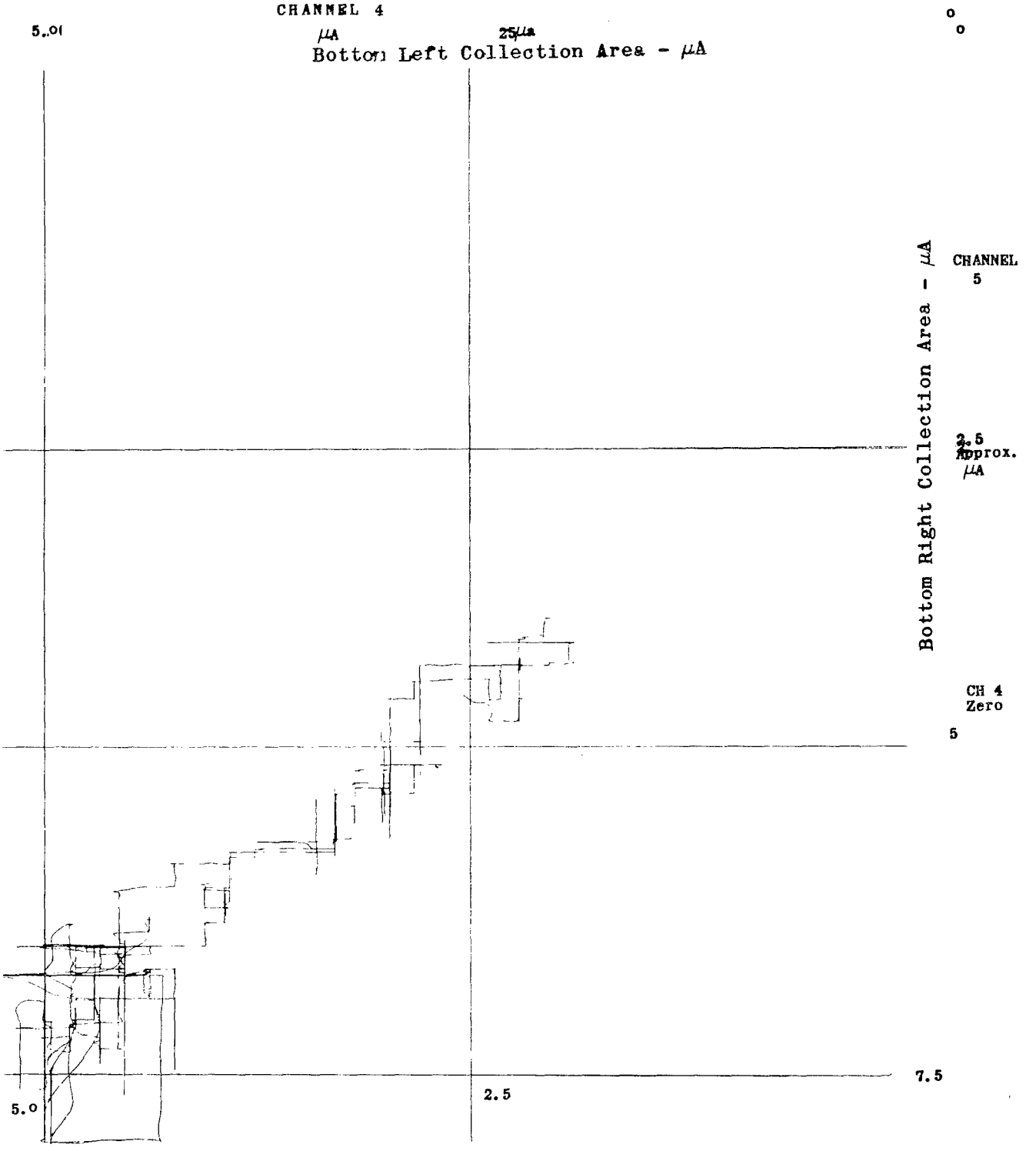

Figure 32
Left Canopy Collector Current as a Function of Right Canopy Collector Current

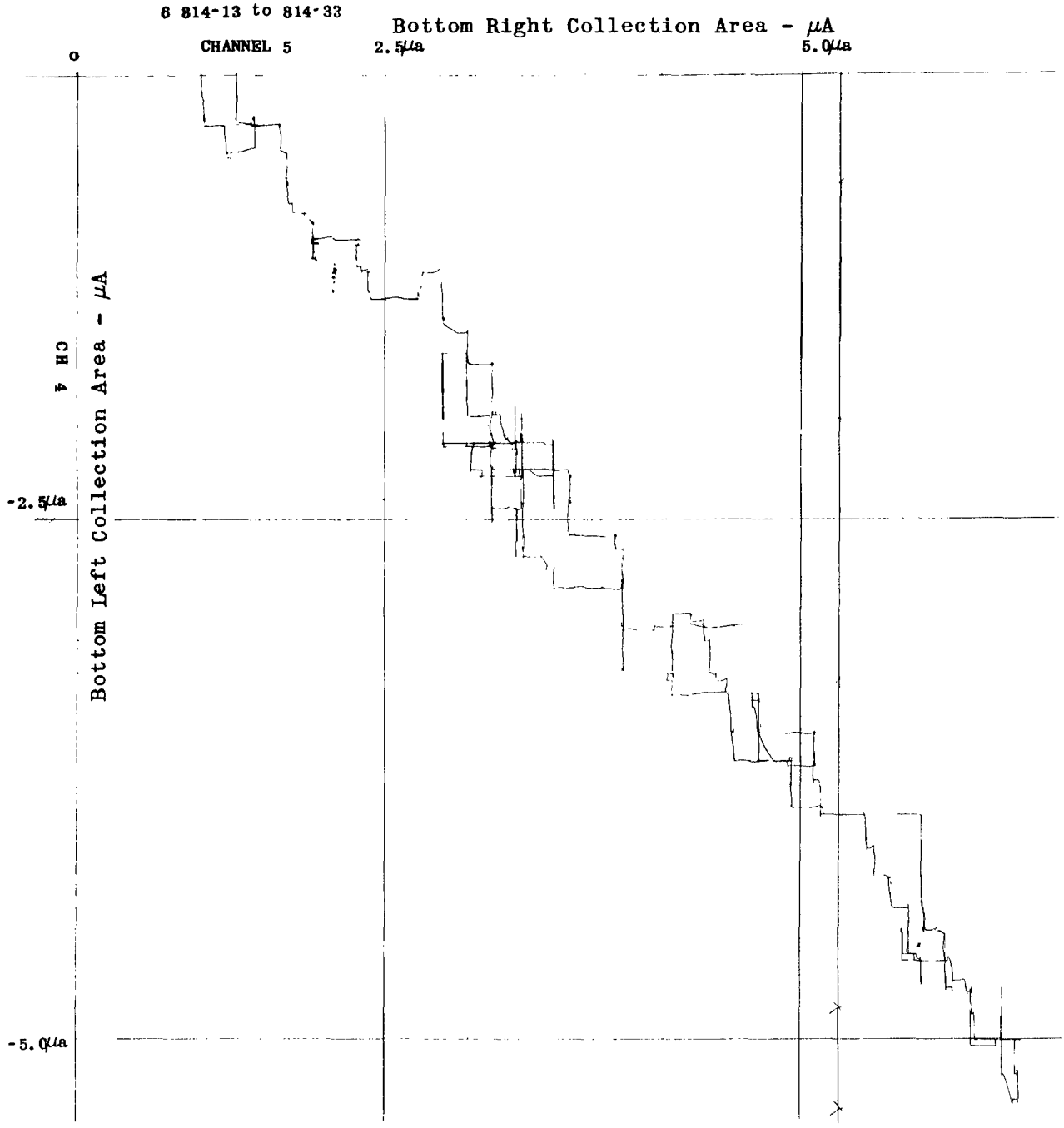

Figure 33
Left Canopy Collector Current as a Function of Right Canopy Collector Current

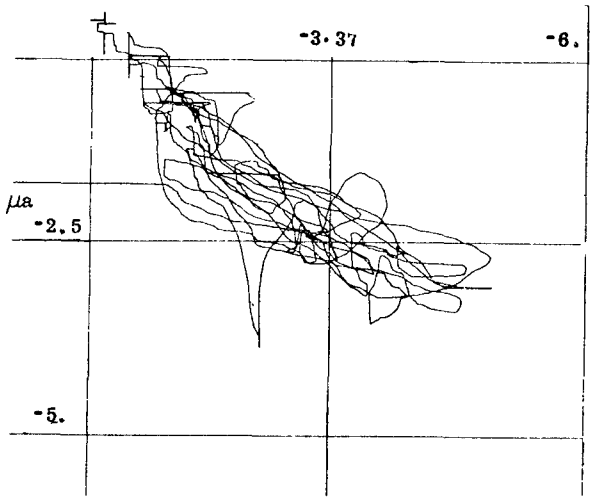

Figure 34
Left Canopy Collector Current as a Function of Right Canopy Collector Current

Table I

Electric Fields Caused by Engine Charging

Location of Field Meter	Magnitude
Top electric field	plus 40 V/cm
Bottom electric field	plus 100 V/cm
Nose electric field	plus 15 V/cm

The positive sign again indicates a positive charge on the airplane. After the fuel modification, no charging was observed which would be attributed directly to engine charging. Negative fields were usually observed on the aircraft immediately after take-off, unless some precipitation was encountered. These fields were of the order of -500 V/cm on the bottom electric field meter, and were attributed to smoke and dust particles in the air close to the ground. No evidence was obtained of momentary reduction of precipitation static by a sudden increase of engine power, as has been reported by pilots.

It is extremely difficult to find sections of oscillograph record with useful data on nose electric field vs noise. In many cases, the nose field will build up to a high value, and remain unchanged for long periods of time. Any measurable change in nose field will ordinarily drive the noise trace off scale or will give such erratic readings that for all quantitative purposes, the data is useless. Two sections of data were analyzed, and Figures 35, page 34 and Figure 36, page 35, show the results. These curves were plotted for small magnitudes of nose field, and relatively low values of noise.

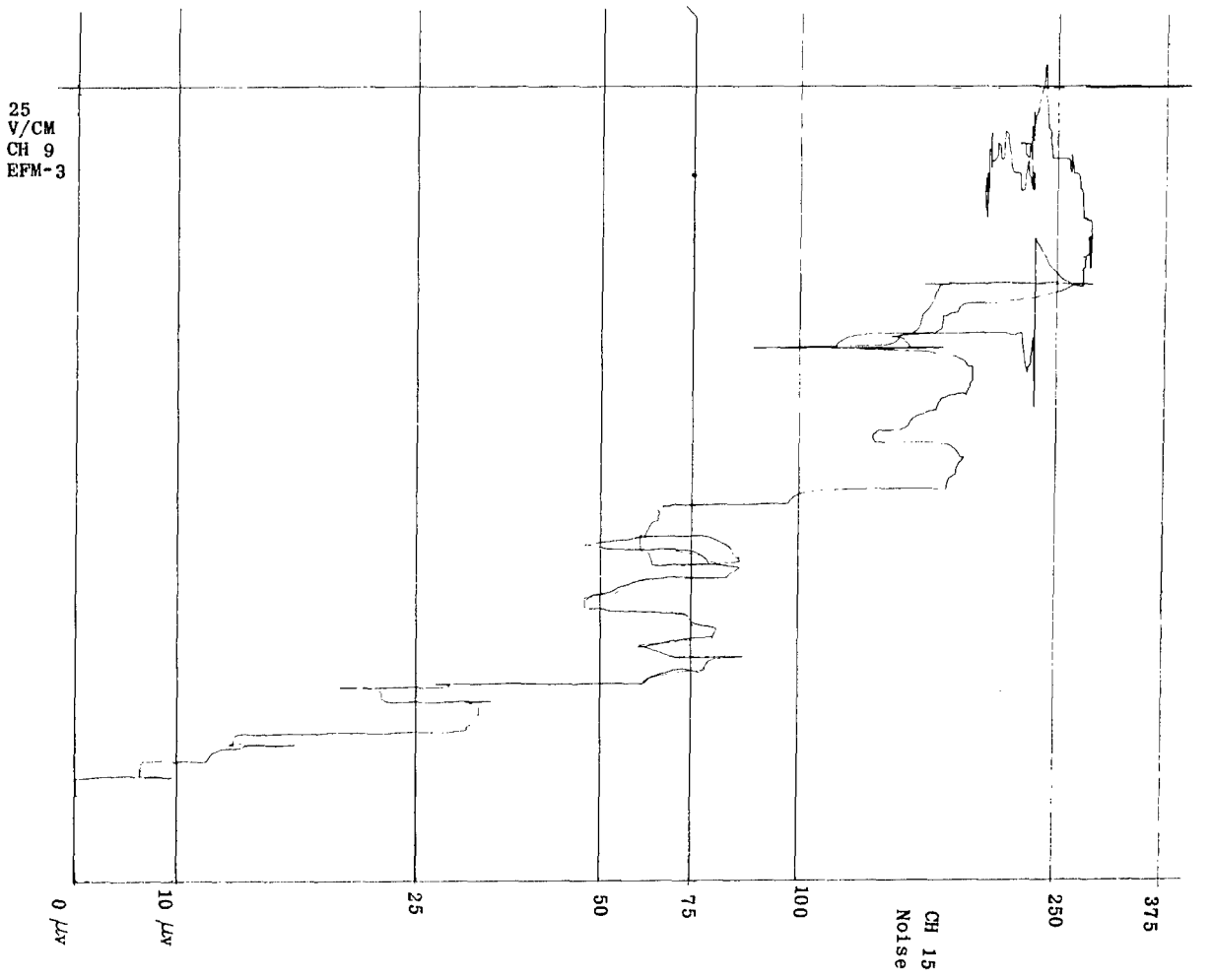

Figure 35
Radio-frequency Noise on the Canopy as a Function of Nose Electric Field

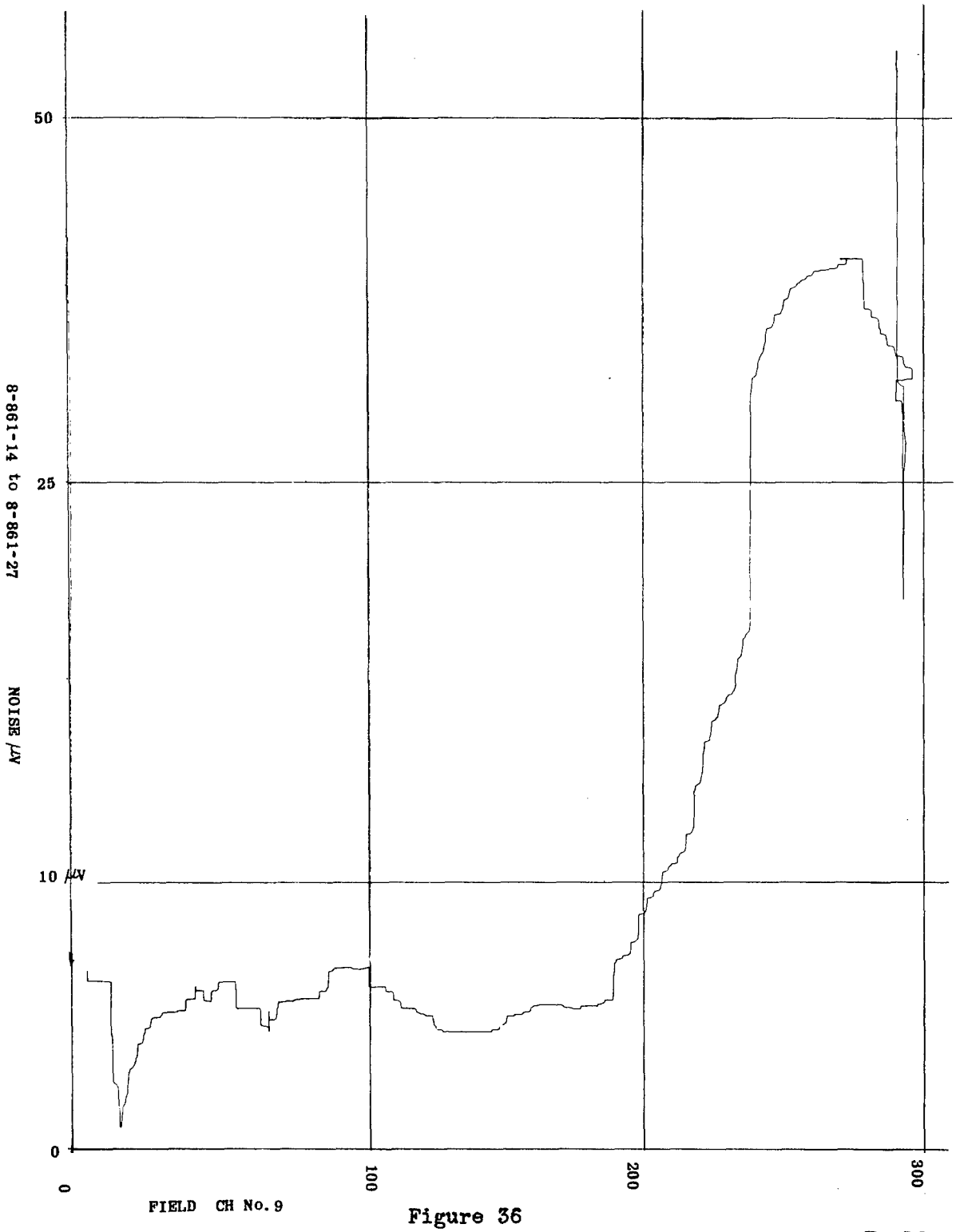

Figure 36
Radio-frequency Noise on the Canopy as a Function of Nose Electric Field

Data were obtained on flight nine, in which the noise level under the canopy went as high as 20,000 microvolts, at a frequency of 300 kc. These data were obtained on a letdown through a cirro-stratus layer at 20 to 25,000 feet at a temperature of about -30°C. The noise was the same under either collection area. Many times during this flight, the noise under the canopy was as great as 5,000 or 10,000 microvolts. The left collection area was treated with a type K-51, antistatic polish sample submitted by Bjorksten Laboratories. Table II shows the noise under the canopy as measured first with one probe, and then with the other.

Table II

R-F Noise Measured on Nose Canopy

Collector Area	Noise	Remarks
Right	1,500 uV	Charging current was decreasing in the interval of measurement
Left	250 uV	
Right	800 to 1,000 uV	
Left	1,000 uV	Charging I -0.85 microamperes*
Right	3,500 uV	Charging I -0.75 microamperes*

*Electric field constant for these two readings

Collector currents were measured at another part of the record, to determine the effect of K-51 treatment on charging currents. The current to the right collection area was negative, while at the same instant, the current to the left collection area was either zero, or slightly positive. At this time, the charging current was very erratic. Table III shows noise measurements on both noise probes. Each pair of readings were taken within one second of each other, which should minimize fluctuations of precipitation density between readings. These data were taken on flight eleven.

Table III

Comparative R-F Noise Measurements on the Noise Probes

Left collector area	Right collector area
4 uV	10 uV
7 or 8 uV	35 uV
4	40 or 50
5	25
5	25
5	15
3	10
5	25

The data obtained on charging current to the nose canopy, electric field under the nose canopy, and noise under the nose canopy are somewhat inconclusive. One reason for this fact is that insufficient flight time in suitable precipitation was obtained. However, sufficient data were obtained to point out the deficiencies in the present instrumentation. These deficiencies are: insufficient sensitivity in the collector current measuring circuit, and insufficient sensitivity in the sense antenna corona current measuring circuit.

A new set of instruments for the airplane has been built which will correct these deficiencies, as well as several others, such as noisy field meter outputs, zero drift in one of the electric field meter circuits, and nonlinearity in all circuits.

SECTION III - CONCLUSIONS

All conclusions are tentative, and are subject to revision when the aircraft becomes available for additional research, and extension of data already obtained.

There is an inherent large scatter in much of the data described in this report. The source of this scatter is lack of information about precipitation density and uniformity, and the lack of closely controlled, known conditions. This scatter prevents the making of any but general statements about empirically derived constants and equations. The material in this report covers a very limited range of magnitudes, and a limited amount of data. For the above reasons, good agreement with data from other sources is not to be expected. However, agreement with other data is good enough on several characteristics to state that jet aircraft are not significantly different from conventional aircraft, except as affected by the higher discharging capacity of jet engines, and higher speeds.

Low-frequency radio noise generated on the outside surface of the canopy, and measured on an antenna under the canopy, is very intense, even under very light charging conditions. This conclusion is further substantiated by the relatively large number of Unsatisfactory Reports received from field installations citing precipitation static failures of radio compass receivers using antennas under or near large non-conducting surfaces.

Additional information is needed on the characteristics and mechanism of canopy charging, and on radio-frequency noise caused by this charging. After this information is obtained, testing of canopy treatments to reduce this noise may be continued on this aircraft.

Additional information is also needed on the general charging characteristics of the aircraft, and on the discharging capacity of jet engines.

[redacted]

BIBLIOGRAPHY

R. C. Ayres and J. O. Jarrard; Aircraft Precipitation Static Investigation; Contract W535-sc-545; T. W. A. Inc.; Aug 1945.

R. C. Ayres; Aircraft Precipitation Static Investigation; Contract W33-106 sc-70; T. W. A. Inc.; Aug 1944.

H. J. Dana; A Final Report on Precipitation Static Reduction Research; Contract OEMsr848; Washington State College; 20 Mar 1944

R. H. George; Final Report on Precipitation Static Tests of Surface Coverings for Aircraft; Purdue Univ. Eng. Expt. Stn.; Contract W33-038 sc-19; 14 July 1945.

Gill & Alfrey; Electrification of Liquid Drops; Nature 163,172(1949).

R. Gunn and W. C. Hall; First Partial Report on the Precipitation Static Problem; Naval Research Lab. Report O-1919; 14 Aug 1942.

R. Gunn, W. C. Hall, and G. D. Kinzler; The Precipitation Static Problem and Methods for its Investigation; Proc. I. R. E. Vol. 34 No. 4, pp 156-161; Apr 1946

R. Gunn and J. P. Parker; The High Voltage Characteristics of Aircraft in Flight; Proc. I. R. E. Vol. 34, No. 5, pp 241-247; May 1946.

Wulf Kunkel; Static Electrification of Dust Particles on Dispersion into a Cloud; Journal of Applied Physics, Aug 1950, 820-832.

I. Langmuir; Final Report on Investigation of Fundamental Phenomena of Precipitation Static; Contract No. W33-106 sc-65; General Electric Co.; May 1945

E. J. Lawton and A. J. Fiumara; Precipitation Static Studies Conducted During a Series of Flights in a B-17 Bomber; Contract No. W33-106 sc-65; Apr 1944.

Leonard B. Loeb; Static Electrification; Univ of Calif. Dept of Physics; Final Report Contract No. N70NR295- Task Order IX Project No. NR 017-201; 2 Sept 1947 to 31 Aug 1950.

Q. J. Porter; Part II, Instrumentation; WADC TR 52-34, Part II, Comm and Nav Laboratory, Weapons Components Division, Wright Air Development Center, Wright-Patterson Air Force Base,*

H. C. Starr; Precipitation Static and Radio Interference Phenomena Originating on Aircraft; Oregon State College Eng. Expt. Stn. Bulletin Series No. 10; June 1939.

*Not published yet.

[redacted]

BIBLIOGRAPHY (Cont'd)

R. G. Stimmel, E. H. Rogers, F. E. Waterfall, and R. Gunn; Electrification of Aircraft Flying in Precipitation Areas; Proc. I. R. E. Vol. 34, No. 4, pp 166-177; April 1946

R. G. Stimmel; Preliminary Investigation of Electrostatic Charging on Jet Aircraft; AMC Engineering Memorandum Report No. MCREE-48-52, 23 Sept 1948; Electronic Subdivision, Communication and Navigation Lab., Wright-Patterson Air Force Base

R. G. Stimmel; Autogenous Electrification of an F-80A Airplane by 14AS-1000 Jato Units. AMC Engineering Memorandum Report No. MCREE-50-25, 2 June 1950; Electronic Subdivision, Comm and Nav Lab., Wright-Patterson Air Force Base

[redacted]

DISTRIBUTION LIST FOR WADC TECHNICAL REPORT 52-34, PART I

Cys	Activities at W-PAFB
3	WCLO
2	WCRR (For Rand Corp.)
10	WCLNT
1	WCAPP
4	BAGR-CD, Mrs. Martin
2	DSC-SA
	Dept. of Defense Activities other Than Those at W-PAFB
1	Commanding Officer Rome Air Development Center ATTN: ENR Griffiss Air Force Base Rome, New York
1	Commanding Officer Air Force Cambridge Research Center ATTN: ERR 230 Albany Street Cambridge 39, Massachusetts
1	Commanding General Strategic Air Command ATTN: Operations Analysis Office Offutt Air Force Base, Nebraska
	Chief of Naval Research Department of the Navy Washington 25, D. C.
6	ATTN: Planning Div., Code N-482
1	ATTN: Elec. Section, Code 427
1	Director U. S. Naval Research Laboratory ATTN: Technical Data Section Washington 25, D. C.

Cys	Activities
1	CO & Director U.S. Navy Electronics Laboratory San Diego 52, California
1	Commanding General Air Research and Development Command ATTN: RDOL P. O. Box 1395 Baltimore 1, Maryland
1	Research and Development Board Library Branch, Information Offices Room 3D1041 The Pentagon Washington 25, D. C.
1	Superintendent United States Naval Academy Post Graduate School Monterey, California
1	Commander U.S. Naval Air Development Center ATTN: Electronics Laboratory Johnsville, Pennsylvania
1	Director of Communications and Electronics Air Defense Command Ent Air Force Base ATTN: AC&W Coordination Division Colorado Springs, Colorado
	Others
1	Beech Aircraft Corporation ATTN: Chief Engineer 6600 East Central Avenue Wichita 1, Kansas

[redacted]

DISTRIBUTION LIST FOR WADC TECHNICAL REPORT 52-34, PART I (Cont'd)

Cys	Organization
2	North American Aviation, Inc. ATTN: Mr. Dave Mason Engineering Data Section Los Angeles International Airport Los Angeles 45, California
3	Northrop Aircraft, Inc. ATTN: Northrop Library, Dept 2135 Hawthorne, California
2	Republic Aviation Corporation ATTN: Engineering Library Farmingdale, New York
1	Airborne Instruments Lab, Inc. ATTN: Mr. E. L. Bock Antenna Section 160 Old Country Road Mineola, Long Island, New York
1	Aircraft Radiation Systems Lab Stanford Research Institute Stanford, California
1	Andrew Alford Consulting Engineers 299 Atlantic Avenue Boston, Massachusetts
1	Antenna Research Laboratory, Inc. ATTN: D. C. Cleckner 709 Thomas Lane Columbus 14, Ohio
1	Mr. R. K. Thomas Research and Development Dept. Bendix Radio Division Baltimore 4, Maryland
1	THRU: District Chief, L. A. Ord Dist. 35 North Raymond Avenue Pasadena 1, California California Institute of Technology Jet Propulsion Laboratory Pasadena, California
1	Dorne and Morgolin Grumman Airfield Bethpage, Long Island, New York
1	Dalmo Victor Company ATTN: Mr. Glen Walters 1414 El Camino Real San Carlos, California
1	Electronics Research, Inc. 2300 N. New York Avenue P. O. Box 327 Evansville, Indiana
1	Applied Physics Laboratory Johns Hopkins University ATTN: Reports Office 8621 Georgia Avenue Silver Spring, Maryland
1	Dr. L. J. Chu Massachusetts Institute of Technology Cambridge 39, Massachusetts
1	The Ohio State University Research Foundation ATTN: Dr. V. H. Rumsey 310 Administration Building Ohio State University Columbus 10, Ohio
1	Raytheon Manufacturing Company ATTN: Dr. H. L. Thomas Documents Section Waltham 54, Massachusetts
1	Stanford Research Institute Stanford, California
2	University of Michigan Aeronautical Research Center ATTN: Mr. L. R. Biasella Willow Run Airport Ypsilanti, Michigan
1	Workshop Associates, Inc. 135 Crescent Road Needham Heights 94, Mass.

DISTRIBUTION LIST FOR WADC TECHNICAL REPORT 52-34, PART I (Cont'd)

Cys	Organization
1	Bell Aircraft Corporation ATTN: Engineering Library L. M. Glass, Librarian Niagara Falls, New York
2	Boeing Airplane Company Seattle Division ATTN: Mr. L. A. Wood Chief, Engineer Seattle 14, Washington
2	Boeing Airplane Company Wichita Division ATTN: Engineering Library Wichita 1, Kansas
1	Chase Aircraft Company, Inc. ATTN: Chief Engineer DeCou and Parkway Avenues Hangar Building 34 Mercer County Airport West Trenton, New Jersey
1	Consolidated-Vultee Aircraft Corp. ATTN: Engineering Library Fort Worth 1, Texas
1	Douglas Aircraft Company, Inc. ATTN: Mr. E. F. Burton Chief Engineer 3000 Ocean Park Boulevard Santa Monica, California
1	Douglas Aircraft Company, Inc. ATTN: Mr. E. H. Heinemann Chief Engineer 827 Lapham Street El Segundo, California
1	Douglas Aircraft Company, Inc. ATTN: Mr. Fred J. Stineman, Chief Engineer 3855 Lakewood Boulevard Long Beach, California
1	Fairchild Engine & Airplane Corp. Fairchild Airplane Division ATTN: L. Fahnestock Hagerstown, Maryland
3	Grumman Aircraft Engineering Corp. ATTN: Chief Engineer Bethpage, Long Island, New York
1	Mr. Sanford Hershfield Electronics Section The Glenn L. Martin Company Baltimore 3, Maryland
3	Hughes Aircraft Company Research & Development Library ATTN: John T. Milek Culver City, California
1	Hughes Aircraft Company ATTN: Mr. N. H. Enenstein Radar Department Culver City, California
	Lockheed Aircraft Corporation Burbank, California
3	Engineering Library, ATTN: Mr. L. Stute
1	ATTN: Mr. H. Rempt
1	The Glenn L. Martin Company ATTN: Engineering Librarian Dr. H. Schutz Baltimore 3, Maryland
1	McDonnell Aircraft Corporation ATTN: Engineering Library P. O. Box 516 Lambert Municipal Airport St. Louis 21, Missouri
1	North American Aviation, Inc. ATTN: Chief Engineer 4300 East Fifth Avenue Columbus 16, Ohio